Metagenomic signature of natural strongyle infection in susceptible and resistant horses

Running head: Parasitic disease and gut microbiome in horses

Allison Clark[1,†], Guillaume Sallé[2, †], Valentine Ballan[3], Fabrice Reigner[4], Annabelle Meynadier[5], Jacques Cortet[2], Christine Koch[2], Mickaël Riou[6], Alexandra Blanchard[2,7], Núria Mach[3*]

[1]Health Science Department, Open University of Catalonia, Barcelona, Spain
[2]UMR 1282, INRA, Infectiologie et Santé Publique and Université François-Rabelais, Nouzilly, France
[3]UMR 1313, INRA, AgroParisTech, Université Paris-Saclay, Jouy-en-Josas, France
[4]UEPAO 1297, INRA, Unité Expérimentale de Physiologie Animale de l'Orfrasière, Nouzilly
[5]UMR 1388, INRA, GenPhySE, Toulouse, France
[6]UE-1277, INRA, Plate-Forme d'Infectiologie Expérimentale, Nouzilly, France
[7] Pancosma SA, CH-1218 Geneva, Switzerland

[†]These authors contributed equally to this work

Corresponding Author:
Núria Mach
Mail: nuria.mach@inra.fr

Word count: 8,587
Figures: 6
Tables: 0

1

Abstract

Gastrointestinal strongyles are a major threat to horses' health and welfare. Given that strongyles inhabit the same niche as the gut microbiota, they may interact with each other. These beneficial or detrimental interactions are unknown in horses and could partly explain contrasted susceptibility to infection between individuals. To address these questions, an experimental pasture trial with 20 worm-free female Welsh ponies (10 susceptible (S) and 10 resistant (R) to parasite infection) was implemented for five months. Fecal egg counts (FEC), hematological and biochemical data, body weight and gut microbiota composition were studied in each individual after 0, 24, 43, 92 and 132 grazing days.

The predicted R ponies exhibited lower FEC after 92 and 132 grazing days, and showed higher levels of circulating monocytes and eosinophils, while S ponies developed lymphocytosis by the end of the trial. Although the overall microbiota diversity remained similar between the two groups, R and S ponies exhibited sustained differential abundances in *Clostridium XIVa, Ruminococcus, Acetivibrio* and unclassified *Lachnospiracea* at day 0. These bacteria may hence contribute to the intrinsic pony resistance towards strongyle infection. Moreover, *Paludibacter*, *Campylobacter, Bacillus, Pseudomonas, Clostridium III, Acetivibrio,* members of the unclassified *Eubacteriaceae* and *Ruminococcaceae* and fungi loads were increased in infected S ponies, suggesting that strongyle and fungi may contribute to each other's success in the ecological niche of the equine intestines. In contrast, butyrate-producing bacteria such as *Ruminococcus, Clostridium XIVa* and members of the *Lachnospiraceae* family decreased in S relative to R ponies. Additionally, these gut microbiota alterations induced changes in several immunological pathways in S ponies, including pathogen sensing, lipid metabolism, and activation of signal transduction that are critical for the regulation of immune system and energy homeostasis. These observations shed light on a putative implication of the gut microbiota in the intrinsic resistance to strongyle infection.

Overall, this longitudinal study provides a foundation to better understand the mechanisms that underpin the relationship between host susceptibility to strongyle infection, immune response and gut microbiota under natural conditions in horses and should contribute to the development of novel biomarkers of strongyle susceptibility and provide additional control options.

1. Introduction

Grazing horses are infected by a complex community of parasitic helminths, manly strongyles (Bucknell et al., 1995; Corning, 2009; Kuzmina et al., 2016; Ogbourne, 1976). Like other worms, strongyles have a direct life cycle in which they can survive outside of its host in pastures as well as in the horse's intestines (Taylor et al., 2007). Infective larvae (L3 stage) are usually ingested and migrate to their preferred niche in the small or large intestine. After two molts, they will eventually become sexually mature adults and will lay eggs that are passed onto the pasture in the feces (Taylor et al., 2007).

Equine strongyle species are classified into *Strongylinae* and *Cyathostominae*, which differ, among other criteria, by their respective size (Lichtenfels et al., 2008). *Strongylus vulgaris* is the most pathogenic of the large strongyles as a result of the intestinal infarction that larval stages can cause during their migration. Its prevalence has been drastically reduced since the release of modern anthelmintics (Nielsen et al., 2012). On the one hand, nearly all horses are

81   infected by small strongyles or cyathostomins throughout the world (Bucknell et al., 1995;
82   Lyons et al., 1999; Ogbourne, 1976). Compared to *S. vulgaris,* small strongyles are
83   responsible for milder symptoms, including weight loss or poor hair condition (Love et al.,
84   1999). Infections are more common in immature animals meaning there is likely an immune
85   component to infection susceptibility (Lyons et al., 1999). Furthermore, larval stages encyst
86   into the colonic mucosa as part of their life cycle where millions can remain for years (Love et
87   al., 1999; Matthews, 2014). Cyathostomin larvae encyst mostly in the autumn and winter in
88   temperate zones of the northern hemisphere, accounting for up to 90% of the total worm
89   burden (Matthews, 2014). The massive emergence of these larvae results in larval
90   cyathostominosis, which is characterized by abdominal pain and diarrhea (Love et al., 1999).
91   Treatment failure in this case can result in the death of horses in at least a third of cases (Giles
92   et al., 1985), underscoring the need for efficient anthelmintic compounds.
93
94   Drug inefficacy reports have accumulated worldwide over the recent years and resistant
95   isolates are now to be found in Europe (Geurden et al., 2014; Sallé et al., 2017), America
96   (Smith et al., 2015) and Oceania (Scott et al., 2015). Additional control strategies are
97   therefore required to alleviate selection pressure put on cyathostomin populations by
98   anthelmintic treatments. One of the possible approaches is to exploit the over dispersion of
99   strongyle infection in a herd to treat the only highly infected horses (Lester and Matthews,
100   2014). Indeed, it has been estimated that 80% of the total worm burden is produced by 20% of
101   horses (Wood et al., 2012) and that 21% of the inter-individual variation had a heritable
102   component (Kornaś et al., 2015). However, the factors underpinning this phenotypic contrast
103   (Lester et al., 2013; Sallé et al., 2015) still remain unclear.
104
105   Equine strongyles are in close contact with a large community of microorganisms in the host
106   intestines, estimated to reach a concentration of 10^9 microorganisms per gram of ingesta in
107   the cecum alone (Mackie and Wilkins, 1988), spanning 108 genera (Mach et al., 2017;
108   Steelman et al., 2012; Venable et al., 2017) and at least seven phyla (Costa et al., 2012, 2015;
109   Mach et al., 2017; Shepherd et al., 2012; Weese et al., 2015). Bacterial populations differ
110   greatly throughout the various compartments of the equine gastrointestinal tract (*e.g*.
111   duodenum, jejunum, ileum and colon) due to differences in the gut pH, available energy
112   sources, epithelial architecture of each region, oxygen levels and physiological roles (Costa et
113   al., 2015; Ericsson et al., 2016). The gut microbiota promotes digestion and nutrient
114   absorption for host energy production and provides folate (Sugahara et al., 2015), vitamin K_2
115   (Marley et al., 1986) and short chain fatty acids (SCFA) such as acetate, butyrate and
116   propionate (Ericsson et al., 2016; Nedjadi et al., 2014). The gut microbiota also neutralizes
117   drugs and carcinogens, modulates intestinal motility, protects the host from pathogens, and
118   stimulates and matures the immune system and epithelial cells (reviewed by Nicholson et al.
119   (2012)). Along with bacteria, both fungi and protozoa, comprise about 6-8% of the equine
120   hindgut population (Dougal et al., 2013).
121
122   The physical presence of helminths in the intestinal lumen can alter the gut microbiota
123   activity and composition (Midha et al., 2017; Peachey et al., 2017). These perturbations have
124   been demonstrated in various host-nematode relationships including mice infected by
125   *Heligmosomoides polygyrus* (Reynolds et al., 2014b; Su et al., 2017), *Nippostrongylus*
126   *brasiliensis* (Fricke et al., 2015)*,* or *Hymenolepis diminuta* (McKenney et al., 2015),
127   ruminants (El-Ashram and Suo, 2017; Li et al., 2011), and pigs (Li et al., 2012; Wu et al.,
128   2012), although no universal modification has been observed across systems. It also remains
129   unresolved whether nematode infection has a beneficial (Lee et al., 2014) or a detrimental
130   (Houlden et al., 2015) impact on the gut microbiota diversity, richness and functions. The

3

131 mechanisms supporting these gut microbiota modifications also remain unclear and could
132 arise indirectly because of the immune response helminths trigger in their host (Cattadori et
133 al., 2016; Fricke et al., 2015; Reynolds et al., 2014b, 2015; Zaiss and Harris, 2016), such as
134 regulatory T cell stimulation and lymphoid tissue modifications, alterations to the intestinal
135 barrier (Boyett and Hsieh, 2014; Giacomin et al., 2016) or directly by the secretion of putative
136 anti-bacterial compounds (Holm et al., 2015; Mcmurdie and Holmes, 2012) or modifications
137 in the intestinal environment that supports them (D'Elia et al., 2009; Midha et al., 2017).
138
139 The putative interactions between equine strongyle infection and the gut microbiota and host
140 physiology are unknown in horses. To address these questions, grazing ponies with extreme
141 resistance or susceptibility toward natural strongyle infection were monitored over a five-
142 month period. We aimed to provide insights into the host response and the gut microbiota
143 composition associated with strongyle natural infection that should guide the development of
144 new microbiota-based control strategies.
145
146 **2. Materials and methods**
147 **2.1. Animals selection**
148 Twenty female Welsh ponies (10 resistant, R, and 10 susceptible, S; 5 ± 1.3 years old) from
149 an experimental unit at the National Institute for Agricultural Research (INRA, UEPAO,
150 Nouzilly, France) were selected from a set of 98 ponies monitored for fecal egg counts (FEC)
151 since 2010. The FEC data were log-transformed to correct for over-dispersion and fitted a
152 linear mixed model accounting for environmental fixed effects (month of sampling, year of
153 sampling, time since last treatment, age at sampling). The individual was considered as a
154 random variable to account for the intrinsic pony potential against strongyle infection.
155 Estimated individual effects were centered and reduced to express each individual potential as
156 a deviation from the mean on the logarithmic scale. Based on these values, two groups of the
157 10 most extreme ponies balanced for age were selected resulting in a resistant R group (mean
158 individual effect with -1.18 phenotypic deviation from the mean and average age of 5.6 years)
159 and a susceptible S group (mean individual effect with +1.45 phenotypic deviation from the
160 mean and average age of 4.7 years). At inclusion, the median FEC was 800 eggs/g for the S
161 group, whereas the median egg counts /g feces was 0 for the R ponies (Figure S1A, S1B and
162 S1C).
163
164 As it has been previously established that gut microbiota profiles might be shaped by host
165 genetics (Goodrich et al., 2014; Lozupone et al., 2012), this information was considered to
166 understand the individual variance underlying microbiota composition. The kinship2 R
167 package was used to create the genetic relationship matrix to estimate the genetic parameters
168 and predicts breeding values between every considered pony. Both pedigree tree and
169 correlation structure matrix are depicted in Figure S1D and Figure S1E, respectively.
170
171 All the procedures were conducted according to the guidelines for the care and use of
172 experimental animals established by the French Ministry of Teaching and Research and the
173 regional Val de Loire Ethics Committee (CEEA VdL, no 19). The protocol was registered
174 under the number 2015021210238289_v4 in the experimental installations with the permit
175 number: C371753. All the protocols were conducted in accordance with EEC regulation (n[o]
176 2010/63/UE) governing the care and use of laboratory animals and effective in France since
177 the 1st of January 2013.
178
179 **2.2. Longitudinal monitoring and sampling**

180   The 20 Welsh ponies were treated with moxidectin and praziquantel (Equest Pramox®,
181   Zoetis, Paris, France, 400 µg/kg of body weight of moxidectin and 2,5 mg/kg of praziquantel)
182   in March 2015 to clear any patent and pre-patent infection and kept indoors for 3 months until
183   the end of the moxidectin remanence period. They were maintained under natural light
184   conditions in a 240 m^2 pen with slatted floors, which precluded further nematode infections
185   until they were moved to the experimental pasture. During housing, animals were fed with
186   hay *ad libitum* and 600 g concentrate per animal per day. The concentrate (Tellus Thivat
187   Nutrition Animale Propriétaire, Saint Germain de Salles, France) consisted of barley (150
188   g/kg), oat bran (162 g/kg), wheat straw (184.7 g/kg), oats (200 g/kg), alfalfa (121.7 g/kg),
189   sugar beet pulp (50 g/kg), molasses (30 g/kg), salt (7.3 g/kg), carbonate Ca (5.5 g/kg) and a
190   mineral and vitamin mix (2 g/kg), on an as-fed basis. The mineral and vitamin mix contained
191   Ca (28.5%), P (1.6%), Na (5.6%), vitamin A (500,000 IU), vitamin D_3 (125,000 IU), vitamin
192   E (1,500 IU), cobalt carbonate (42 mg/kg), cupric sulfate (500 mg/kg), calcium iodate (10
193   mg/kg), iron sulfate (1,000 mg/kg), manganese sulfate (5,800 mg/kg), sodium selenite (16
194   mg/kg), and zinc sulfate (7,500 mg/kg) on an as-fed basis.
195
196   Grazing started by the end of a 3-month moxidectin remanence period (mid-June 2015).
197   Ponies grazed from mid-June to the end of October 2015 at the Nouzilly experimental station
198   (France). The experimental pasture (7.44 ha) consisted of tall fescue, *Festuca arundinacea*;
199   timothy-grass, *Phleum prateonse*, meadow-grass, *Poa abbreviata*; soft-grass, *Holcus lanatus*;
200   and cocksfoot, *Dactylis glomerata*). During all phases of the experimental period, ponies were
201   provided *ad libitum* access to water.
202
203   Moxidectin is known to have moderate efficacy against encysted cyathostomin larvae
204   (Reinemeyer et al., 2015; Xiao et al., 1994). Therefore, residual egg excretion can occur at the
205   end of the remanence period, as a result of encysted larvae completing their development into
206   adults. To eliminate this residual excretion and to avoid any interference with strongyle
207   infection at pasture, a treatment targeting the only luminal immature and adult stages
208   (pyrantel embonate; Strongid® paste, Zoetis, Paris, France; single oral dose of 1.36 mg
209   pyrantel base per Kg of body weight) was implemented at day 30.
210
211   Every pony was subjected to a longitudinal monitoring of fecal strongyle egg excretion and
212   microbiota was performed monthly, *e.g.* 0, 24, 43, 92 and 132 days after the onset of grazing
213   (Figure 1).
214
215   Fecal samples were collected from the rectum. Fecal aliquots for microbiota analysis were
216   immediately snap-frozen in liquid nitrogen and stored at -80°C until DNA extraction, whereas
217   fecal aliquots to measure the fecal egg counts were immediately sent to the laboratory.
218   The pH in the feces was immediately determined after 10% fecal suspension (wt/vol) in saline
219   solution (0.15 M NaCl solution).
220
221   Blood samples were taken from each pony and collected in EDTA-K3-coated tubes (5 mL) to
222   determine hematological parameters and heparin tubes (10 mL) to determine biochemical
223   parameters. After clotting, the heparin tubes were centrifuged at 4000 rpm during 15 min and
224   the harvested plasma was stored at -20°C until analysis. Additionally, blood collected in
225   EDTA-K3-tubes was used to measure the different blood cells.
226
227   For each individual, body weight and average daily weight gain were recorded until the end of
228   the experiment.
229

230 None of the ponies received antibiotic therapy during the sampling period and diarrhea was
231 not detected in any ponies.
232
233 **2.3. Fecal egg counts**
234 Fecal egg counts (eggs per gram of wet feces) was measured as a proxy for patent strongyle
235 infection. FEC was carried out using a modified McMaster technique (Raynaud, 1970) on 5 g
236 of feces diluted in 70 mL of NaCl solution with a density of 1.2 (sensitivity of 50 eggs/g). A
237 Wilcoxon rank-sum test with Benjamini-Hochberg multiple test correction was used to
238 determine whether there was a significant difference between groups across the experiment. A
239 $q < 0.05$ was considered significant.
240
241 **2.4. Blood hematological and biochemical assays**
242 For blood hematological assays, blood were stirred at room temperature for good oxygenation
243 during 15 min. Different blood cells were analyzed, including leucocytes (lymphocytes,
244 monocytes, neutrophils, basophils and eosinophils), erythrocytes and different blood
245 parameters such as hematocrit, mean corpuscular volume and the thrombocytes. The total
246 blood cells were counted with a MS9-5 Hematology Counter® (digital automatic hematology
247 analyzer, Melet Schloesing Laboratories, France).
248 The serum biochemical parameters (albumin, cholesterol, globin, glucose, phosphatase
249 alkaline, total proteins and urea) were measured colorimetric method using Select-6V rings
250 with the M-ScanII Biochemical analyzer (Melet Schloesing Laboratories, France).
251
252 Mixed-effects analysis of the variance (ANOVA) or Wilcoxon rank-sum tests were conducted
253 for continuous variables fitting a normal or non-normal distribution respectively to delineate
254 whether there was a significant difference between the average values of phenotype traits for
255 the different groups, using a significance level of $p < 0.05$. Blood cell counts were corrected
256 for the mild dehydration by fitting the hematocrit as a co-variable in the model.
257
258 **2.5. Weather data**
259 Daily precipitation and temperatures were recorded at a meteorological station located 14 km
260 from the experimental area.
261
262 **2.6. Pasture contamination**
263 Pasture contamination was assessed before the entry to the pasture and during the experiment.
264 The number of infective larvae (L3) per kg of dry herbage was measured by 100 x 4 random
265 sampling of grass on pasture following previously described method (Gruner and Raynaud,
266 1980). First, 600 g of grass were mixed with 20 mL of neutral pH soap diluted in 5L of tap
267 water to allow larvae migration. This solution was subsequently left at room temperature prior
268 to washing for larval recovery. Second, the washed material was passed through a coarse
269 mesh sieve (20 cm of diameter) and collected in a container, then passed through both a 125
270 µm mesh sieve and a 20 µm mesh sieve. Third, the solution of the filtered material was split
271 into four 10 mL glass tubes before centrifugation at 2500 rpm for 5 min. Water was soaked
272 and replaced by a dense solution (NaCl, density 1.18-1.2). Lastly, a cover slip was added on
273 the top of each. Tubes were subsequently centrifuged gently at 1500 rpm for 8 min to allow
274 larval material adhere onto the cover slip, before further examination under an optical
275 microscope. This step was performed four times.
276
277 **2.7. Pasture chemical analysis**
278 Hay was sampled at day 0 via grab samples from multiple depths into a bale and then
279 composited. Herbage samples were collected from three randomly selected zones in the

280   experimental pasture at days 24, 43, 92 and 132. At each sampling time, 10 hand-plucked
281   samples simulating « bites » were taken from pasture. All samples were frozen until chemical
282   analyses. Chemical compositions of samples were determined according to the "Association
283   Française de Normalisation" (AFNOR) procedures: NF V18-109 (AFNOR, 1982) for dry
284   matter (DM); NF V18-101 (AFNOR, 1977b) for crude ash; NF V18-100 (AFNOR, 1977a) for
285   crude proteins; NF V03-040 (AFNOR, 1993) for crude fiber; NF V18-117 (AFNOR, 1977a)
286   for crude fat; NF V18-122 (AFNOR, 1997) for neutral detergent fiber (NDF), acid detergent
287   fiber (ADF) and acid detergent lignin (ADL). All of them were assayed with a heat stable
288   amylase and expressed with exclusive of residual ash according to the method of Van Soest et
289   al. (1991). Non-fiber carbohydrate (NFC), also called neutral detergent soluble carbohydrate
290   (NDCS) were obtained by calculations: NFC = 1000 – CP – CF – Mm – NDF.
291

292   **2.8. Microorganisms DNA extraction from feces samples**
293   Total DNA was extracted from aliquots of frozen fecal samples (200 mg; 100 samples at
294   different time points from 20 ponies), using E.Z.N.A.® Stool DNA Kit (Omega Bio-Tek,
295   Norcross, Georgia, USA). The DNA extraction protocol was carried out according to the
296   manufacturer's instructions (Omega- Bio-Tek, Norcross, Georgia, USA).
297

298   **2.9. V3–V4 16S rRNA gene amplification**
299   The V3-V4 hyper-variable regions of the 16S rDNA gene were amplified with two rounds of
300   PCR using the forward primer (5'-
301   CTTTCCCTACACGACGCTCTTCCGATCTACGGRAGGCAGCAG-3') and the reverse
302   primer (5'- GGAGTTCAGACGTGTGCTCTTCCGATCTTACCAGGGTATCTAATCCT-3')
303   modified in order to include Illumina adapters and barcode sequences which allow for
304   directional sequencing. The first round of amplification was performed in triplicate in a total
305   volume of 50 μL containing 10 ng of DNA, 2.5 units of a DNA-free Taq DNA Polymerase
306   and 10X Taq DNA polymerase buffer (MTP Taq DNA Polymerase, Sigma). Subsequently, 10
307   mM of dNTP mixture (Euromedex, Souffelweyersheim, France), 20 mM of each primer
308   (Sigma, Lezennes, France) and Nuclease-free water (Ambion, Thermo Fisher Scientific,
309   Waltham, USA) were added. Ultrapure Taq DNA polymerase, ultrapure reagents, and plastic
310   were selected in order to be DNA-free. The thermal cycle consisted of an initial denaturation
311   step (1 min at 94°C), followed by 30 cycles of denaturation (1 min at 94°C), annealing (1 min
312   at 65°C) and 1 min of extension at 72°C. The final extension step was performed for 10 min
313   at 72°C. Amplicons were then purified using magnetic beads (Clean PCR system, CleanNA,
314   Alphen an den Rijn, The Netherlands) as follows: beads/PCR reactional volume ratio of 0.8X
315   and final elution volume of 32 μL using Elution Buffer EB (Qiagen). The concentrations of
316   the purified amplicons were checked using a NanoDrop 8000 spectrophotometer (Thermo
317   Fisher Scientific, Waltham, USA).
318

319   Sample multiplexing was performed thanks to 6 bp unique indexes, which were added during
320   the second PCR step at the same time as the second part of the P5/P7 adapters used for the
321   sequencing step on the Illumina MiSeq flow cells with the forward primer (5'-
322   AATGATACGGCGACCACCGAGATCTACACTCTTTCCCTACACGAC-3') and reverse
323   primer (5'-
324   CAAGCAGAAGACGGCATACGAGATNNNNNNGTGACTGGAGTTCAGACGTGT-3').
325   This second PCR step was performed using 10 ng of purified amplicons from the first PCR
326   and adding 2.5 units of a DNA-free Taq DNA Polymerase and 10X MTP TaqDNA
327   polymerase buffer (Sigma). The buffer was complemented with 10 mM of dNTP mixture
328   (Euromedex), 20 mM of each primer (Eurogentec, HPLC grade) and Nuclease-free water
329   (Ambion, Life Technologies) up to a final volume of 50 μL. The PCR reaction was carried

330 out as follows: an initial denaturation step (94°C for 1 min), 12 cycles of amplification (94°C
331 for 1 min, 65°C for 1 min and 72°C for 1 min) and a final extension step at 72°C for 10 min.
332 Amplicons were purified as described for the first PCR round. The concentration of the
333 purified amplicons was measured using Nanodrop 8000 spectrophotometer (Thermo
334 Scientific) and the quality of a set of amplicons (12 samples per sequencing run) was checked
335 using DNA 7500 chips onto a Bioanalyzer 2100 (Agilent Technologies, Santa Clara, CA,
336 USA). All libraries were pooled at equimolar concentration in order to generate equivalent
337 number of raw reads with each library. The final pool had a diluted concentration of 5 nM to
338 20 nM and was used for sequencing. Amplicon libraries were mixed with 15% PhiX control
339 according to the Illumina's protocol. Details on sequencing, PhiX control and FastQ files
340 generation are specified elsewhere (Lluch et al., 2015). For this study, one sequencing run
341 was performed using MiSeq 500 cycle reagent kit v2 (2x250 output; Illumina, USA).
342
343 **2.10. Sequencing Data Preprocessing**
344 Sequences were processed using the version 1.9.0 of the Quantitative Insights Into Microbial
345 Ecology (QIIME) pipeline (Caporaso et al., 2010; Rideout et al., 2014) and by choosing the
346 open-reference operational taxonomic units (OTU) calling approach (Rideout et al., 2014).
347 First, forward and reverse paired-end sequence reads were collapsed into a single continuous
348 sequence according to the 'fastq-join' option of the 'join_paired_ends.py' command in
349 QIIME. The fastq-join function allowed a maximum difference within overlap region of 8%,
350 a minimum overlap setting of 6 bp and a maximum overlap setting of 60 bp. The reads that
351 did not overlap (~20% of the total) were removed from the analysis. The retained sequences
352 were then quality filtered. De-multiplexing, primer removal and quality filtering processes
353 were performed using the 'split_libraries'_fastq.py command in QIIME. We applied a default
354 base call Phred threshold of 20, allowing maximum three low-quality base calls before
355 truncating a read, including only reads with >75% consecutive high-quality base calls, and
356 excluding reads with ambiguous (N) base calls (Navas-Molina et al., 2013).
357 Subsequently, the sequences were clustered into OTUs against the GreenGenes database
358 (release 2013-08: gg_13_8_otus) (DeSantis et al., 2006) by using the uclust (Edgar, 2010)
359 method at a 97% similarity cutoff. The filtering of chimeric OTUs was performed by using
360 Usearch version 6.1 (Edgar et al., 2011) against the GreenGenes reference alignment
361 (DeSantis et al., 2006). A phylogenic tree was generated from the filtered alignment using
362 FastTree (Price et al., 2010). Singletons were discarded from the dataset to minimize the
363 effect of spurious, low abundance sequences using the 'filter_otus_from_otu_table.py' script
364 in QIIME. To confirm the annotation, the resulting OTU representative sequences were then
365 searched against the Ribosomal Database Project naïve Bayesian classifier (RDP 10 database,
366 version 6 (Cole et al., 2009) database, using the online program SEQMATCH
367 (http://rdp.cme.msu.edu/seqmatch/seqmatch_intro.jsp). Finally, consensus taxonomy was
368 provided for each OTU based on the taxonomic assignment of individual reads using
369 GreenGenes and RDP databases. Using OTU abundance and the corresponding taxonomic
370 classifications, feature abundance matrices were calculated at different taxonomic levels,
371 representing OTUs and taxa abundance per sample. The "Phyloseq" (Mcmurdie and Holmes,
372 2012) and "Vegan" (Dixon, 2003) R package were used for the detailed downstream analysis
373 on abundance matrix.
374
375 In the end, a total of 8,010,052 paired-end 250 bp reads were obtained, 6,428,315 of which
376 were retained as high-quality sequences (Table S1). On average, a total of 58,015 sequences
377 per sample were obtained in the study, with a mean length of 441 ± 15 bp. These sequences
378 were clustered into 15,784 OTUs using the reference-based OTU-picking process (Table S2).
379 Among them, 12,069 were classified taxonomically down to the genus level (Table S2). OTU

380   counts per sample and OTU taxonomical assignments are available in Table S2. We filtered
381   out unclassified taxa from the analysis because the main goal of the current study was to
382   identify specific taxa related to host susceptibility to strongyle infection.
383
384   The α-diversity indexes (observed species richness, Chao1(Chao, 1984) and Shannon
385   (Shannon, 1997)) were calculated using the "Phyloseq" R package (Mcmurdie and Holmes,
386   2012). Shannon's diversity index is a composite measure of richness (number of OTUs
387   present) and evenness (relative abundance of OTUs). The nonparametric Wilcoxon rank-sum
388   test was used to compare α-diversity indexes between groups.
389
390   Relative abundance normalization was applied, which divides raw counts from a particular
391   sample by the total number of reads in each sample.
392
393   To estimate β-diversity, un-weighted and weighted UniFrac distances were calculated from
394   the OTU and genera abundance tables, and used in principal coordinates analysis (PCoA),
395   correspondence analysis (CA), and non-parametric multidimensional scaling (NMDS) with
396   the "Phyloseq" R package. The Permutational Multivariate Analysis of Variance
397   (PERMANOVA), on un-weighted and weighted UniFrac distance matrices were applied
398   through the Adonis function from "Vegan" R package to test for groups effect. In addition to
399   multivariate analysis, we used the analysis of similarities (ANOSIM) to test for intragroup
400   dispersion. ANOSIM is a permutation-based test where the null hypothesis states that within-
401   group distances are not significantly smaller than between-group distances. The test statistic
402   (R) can range from 1 to –1, with a value of 1 indicating that all samples within groups are
403   more similar to each other than to any other samples from different groups. R is ≈0 when the
404   null hypothesis is true, that distances within and between groups are the same on average.
405
406   The Wilcoxon rank-sum test with Benjamini-Hochberg multiple test correction was used to
407   determine the differentially abundant OTUs, phyla, families, and genera between groups. A
408   $q < 0.25$ was considered significant. This threshold was employed in previous microbiome
409   studies because allows compensation for the large number of microbial taxa and multiple
410   comparison adjustment (Lim et al., 2017).
411
412   This targeted locus study project has been deposited at DDBJ/EMBL/GenBank under the
413   accession KBTQ01000000. The version described in this paper is the first version,
414   KBTQ01000000. The bioproject described in this paper belongs to the BioProject
415   PRJNA413884. The corresponding BioSamples accession numbers were SAMN07773451 to
416   SAMN07773550.
417
418   **2. 11. Functional metagenomic predictions**
419   The functional prediction for the 16S rRNA marker gene sequences was done using the
420   phylogenetic investigation of communities by reconstruction of unobserved states
421   (PICRUSt) (Langille et al., 2013). After excluding the unknown OTUs from the GreenGenes
422   reference database and normalizing by 16S rRNA gene copy number, functional
423   metagenomes for each sample were predicted from the Kyoto Encyclopedia of Genes and
424   Genomes (KEGG) catalogue and collapsed to a specified KEGG level. We used Wilcoxon
425   rank-sum test with Benjamini-Hochberg multiple test correction to evaluate pathway-level
426   enrichments between groups. A $q < 0.05$ was considered as significant.
427
428   **2.12. Network inference at the genus level**

429   Networks at the genus level were inferred between groups at different time points. In order to
430   prevent the compositional effects bias typical of the classical correlations methods, we
431   calculated the correlations among genera using the PCIT method, which identifies significant
432   co-occurrence patterns through a data-driven methodology based on partial correlation and
433   information theory as implemented in the PCIT algorithm (Reverter and Chan, 2008). Further
434   details are depicted in Ramayo-Caldas et al. (2016). The genera with < 0.1% mean relative
435   abundances were excluded to acquire the results for the taxa that met the statistical conditions
436   for correlation estimations. Nodes in the network represent the genera and edges that connect
437   these nodes represent correlations between genera. Based on correlation coefficient and *p*-
438   values for correlation, we constructed co-occurrence networks. The cutoff of *p*-values was
439   0.05. The cutoff of correlation coefficients was determined as r≥|0.35|. Network properties
440   were calculated with the NetworkAnalyzer plugin in Cytoscape. We used the "iGraph" R
441   package to visualize the network. Strong and significant correlation between nodes (r≥|0.60|)
442   were represented with larger edge width in the network.
443
444   **2.13. Real-time quantitative PCR (qPCR) analysis of bacterial, fungal and protozoan**
445   **loads**
446   Loads of protozoa, anaerobic fungi and bacteria in fecal samples were quantified using a
447   QuantStudio 12K Flex real-time instrument (Thermo Fisher Scientific, Waltham, USA).
448   Primers for real-time amplification of ciliates, anaerobic fungi and bacteria have already been
449   described in Mach et al. (2017) and have been purchased from Eurofins Genomics
450   (Ebersberg, Germany).
451   Amplified fragments of the target genes were used and diluted 10-fold in series to produce
452   seven standards, ranging from 2.25×10^7 to 2.25×10^{13} copies per μg of DNA for bacteria
453   and protozoa and ranging from 3.70×10^6 to 3.70×10^{12} copies per μg of DNA for ciliates and
454   fungi. Each reaction contained, in a final volume of 20 μL, 10 μL of Sybergreen Mix (Power
455   SYBR Green PCR Master Mix, ThermoFisher, Ullkirch-Graffenstaden, France), 0.6 μM of
456   each primer to final concentration of 300 mM, and 2 μL of standard or DNA template at 0.5
457   ng/μL. The primer concentration of anaerobic fungi was 200 mM and 150 mM for ciliate
458   protozoa. The DNA template was 0.5 ng/μL. In all cases, the thermal protocol for qPCR
459   amplification and detection included an initial step of denaturation of 10 min (95 °C),
460   followed by 40 amplification cycles [15 s at 95 °C; 60 s at 60 °C]. After each run, melting
461   curves between 60 and 95 °C were evaluated to confirm the absence of unspecific signals. For
462   each sample and each gene, qPCR runs were performed in triplicate. The standard curve
463   obtained the reference genomic fragment was used to calculate the number of copies of
464   bacteria, protozoa or anaerobic fungi in feces. Taking into account the molecular mass of
465   nucleotides and fragment length, we calculated the copy number as follows: mass in Daltons
466   (g/mol) = (size of double-stranded [ds] product in base pairs [bp]) (330 Da × 2 nucleotides
467   [nt]/bp). Wilcoxon rank-sum tests were calculated for all possible group combinations. A *p*
468   < 0.05 was considered significant.
469
470   **3. Results**
471   The effects of natural strongyle infection on gut microbiota composition and host phenotypic
472   variables were determined in ten resistant and ten susceptible grazing ponies over a five-
473   month grazing season (Figure 1). Metagenomic, parasitological, hematological and
474   biochemical measures were performed at five time points (Figure S2), hereafter referred to as
475   days after the onset of the grazing season or grazing days (gd).
476
477
478

3.1. A mixture of abiotic and biotic environmental stressors during the 43-day transitioning period induced shifts in immunological and microbiota profiles

Measured FEC demonstrated a residual egg excretion in one susceptible individual at day 0 and in two susceptible ponies after 24 gd (Figure 2A and 2B). This was due to the known imperfect efficacy of moxidectin against encysted stages of strongyle. Because we were interested in studying the effects of strongyle exposure on the gut microbiota, a pyrantel treatment was administered after 30 gd to reset luminal parasite stages to zero in every pony. This treatment has a short-lived effect and resulted in negative FECs at 43 gd (Figure 2A and 2B). Therefore, the 0-43 gd period was considered as a transitioning period resulting in both, mild parasite exposure and changes in environmental conditions.

Indeed, a heat wave took place over the first 43 days of the trial resulting in almost no rainfall (0.2 mm) and high temperatures peaking at 37.7 ºC (Figure S3A). This situation ultimately led to grass senescence and lowered pasture quality (Figure S3B, Table S3). Mild dehydration also occurred in ponies as supported by a constant rise in measured hematocrits from 32.33 to 39.63 % during the first 43 gd (Figure 2C). To account for this, blood cell counts were corrected by hematocrit through time. Recorded hematological data showed that ponies were neither anemic nor thrombocytopenic throughout the experiment (Figure S4).

Concomitantly to these challenging conditions, increased levels of some white blood cell populations were observed, namely eosinophils (2.75-fold increase, $p = 5.98$ x 10^{-13}, Figure 2D), and monocytes (1.64-fold increase, $p = 2.94$ x 10^{-7}; Figure 2E) during the first 43 gd. Notably, R ponies had significantly higher levels of these immunological cells from 24 to 43 gd relative to S ponies. Grass samples analysis did not evidence any infective larvae until 43 gd.

16S rRNA gene sequencing was used to profile the fecal microbiota of the S and R ponies across time. Despite the distinctive susceptibility to parasite infection, the overall community structure showed no statistically significance difference in un-weighted (presence/absence) Unifrac analysis (PERMANOVA, $p > 0.05$) or abundance-weighted analysis (PERMANOVA, $p > 0.05$) during the first 43 days of the experiment. Measures of α-diversity (Chao1 richness, observed species and Shannon diversity index) were not significantly different between the two groups (Wilcoxon rank-sum test, $p > 0.05$). Although the overall gut microbial community of S ponies during the first 43 days of experiment was almost indistinguishable from those of R ponies, we next evaluated the association between the abundance of specific gut microbial taxa and the susceptibility to parasite infection. Statistical differences were not evident at phylum and family levels (Figure 3A). Only seven genera were statistically significant at a nominal p value < 0.05 (Wilcoxon rank-sum test; Figure 3B and 3C, Table S4) at day 0, including *Acetivibrio*, *Clostridium XIVa*, *Ruminococcus*, *Halella*, *Syntrophococcus*, unclassified *Lachnospiracea*, and *Lachnospiracea incertae sedis*, whereas a total of 20 taxa had differential presence at a nominal p value < 0.05 at day 24 (Wilcoxon rank-sum test; Figure 3C, Table S4). Specifically, species belonging to the *Blautia* and *Paraprevotella* genera were relatively more abundant ($p < 0.05$) in the S group compared to the R group (Table S4) at 24 gd. Conversely, other genera belonging to the Clostridiales order (*e.g. Clostridium sensu stricto, Clostridium IV, Clostridium III, Syntrophococcus, Oribacterium, Dehalobacterium, Mogibacterium, Acetivibrio*, *Sporobacter* and unclassified *Ruminococcaceae*) and Bacteroidales (*e.g. Hallella, Rikenella, Paraprevotella* and *Bacteroides*) were more abundant in the R group than in the S group at 24 gd (Figure 3B). These shifts in microbial taxa were not associated with modifications in functional gene abundances, as predicted from 16*S* rRNA data analysis ($q > 0.05$; Table S5).

11

3.2. The predicted levels of resistance matched observed fecal egg counts between resistant and susceptible ponies and shifts in the gut microbiota composition.

By the end of the transition period, *e.g.* after 43gd, ponies were considered adapted to their new environmental conditions. The resetting of luminal stages with pyrantel resulted in negative FEC across ponies at 43 days after the onset of grazing (Figure 2A and 2B). After the patent infection, parasite egg excretion was significantly higher in the susceptible group after 92 (235 eggs in S and 20 eggs in R ponies on average) and 132 gd (340 eggs in S and 135 eggs in R ponies on average; Figure 2A).

The ponies' body weights (Figure S5A) and average daily weight gains (Figure S5B) did not show significant differences between groups after natural parasite infection, and none of them displayed clinical symptoms like lethargy or diarrhea. However, strongyle exposure induced contrasted shifts in white blood cell populations between the two groups of ponies. Circulating monocyte levels were higher ($p < 0.05$) in R in comparison to S ponies through the whole period (Figure 2E). But the opposite trend was found for circulating lymphocytes, which were significantly enriched in the white blood cells population in S ponies during parasite infection (Figure 2F). Among the white blood cell population, R ponies also presented higher levels of eosinophils at 132 gd ($p < 0.05$, figure 2D). Similarly, serum biochemical analyses revealed a mild elevation in albumin, cholesterol, the enzyme alkaline phosphatase and total proteins from 43 gd to the end of the experiment in both groups, as well as elevated levels of urea, in particular at 92 and 132 gd (Figure S6).

Strongyle mediated alterations in microbiota diversity and structure were investigated between the two groups of ponies. As for the transition period, both groups of ponies displayed equivalent microbial species richness and alpha-diversity indexes (Wilcoxon rank-sum test, $p > 0.05$, Figure 4A). The diversity Chao1 and Shannon indexes were similar between the two groups through time (Wilcoxon rank-sum test, $p > 0.05$, Figure 4B). The UniFrac distance followed by PCoA (Figure 4C) showed no distinct clustering between samples from the S and the R group, which was indicative of, if at all, minor differences in microbiota composition between the two groups of ponies during parasite infection. Similarly, the correspondence analysis (Figure 4D) and the Jaccard network (Figure 4E) analyses suggested that the overall gut microbiota composition was largely similar between S and R ponies at each time point.

However, changes in relative abundance of certain genera concomitantly arose with strongyle egg excretion at 92 gd. For example, *Paludibacter*, *Campylobacter, Bacillus, Pseudomonas, Clostridium III, Acetivibrio,* and members of the unclassified family *Eubacteriaceae* and *Ruminococcaceae* increased in S relative to R ponies ($p < 0.05$ and $q \leq 0.25$; Figure 3C). Moreover, the relative abundance of *Acetivibrio,* and *Clostridium* III highly correlated with FEC (Pearson correlation coefficient $\rho > 0.60$). This genera enrichment was concomitant with depletion in *Ruminococcus, Clostridium XIVa* and members of the *Lachnospiraceae* family ($p < 0.05$ and $q \leq 0.25$, Figure 3C). The complete list of differentially expressed genera and q-values is presented in Supplementary Table S4. These modifications in the gut bacterial community structure between S and R also resulted in functional modifications, as inferred from PICRUSt. Noteworthy, among the well-characterized bacterial functions, S ponies microbiota tended to show an enrichment ($q < 0.10$) of the mineral absorption, protein digestion and absorption, as well as of some of the pathways related to cell motility (*e.g.* bacterial chemotaxis, bacterial motility proteins, flagellar assembly), lipid metabolism (sphingolipid metabolism), peroxisome, and signal transduction (phosphatidylinositol signaling system) among others compared to the R group at 92 gd (Table S5).

12

579 Because the magnitude and direction of changes for *Clostridium XIVa, Ruminococcus,*
580 *Acetivibrio* and unclassified *Lachnospiracea* observed at 92 gd between the two groups were
581 already remarked at day 0, we evaluated the host genetics. Interestingly, 80% of the ponies
582 from group R presented higher genetic relatedness (Figure S1E), whereas there was no
583 evidence for high genetic relatedness between S individuals.
584
585 The gut microbiota co-occurrence networks were marginally different between S and R
586 ponies at 92 gd (Figure S7). The topological properties were calculated to describe the
587 complex pattern of inter-relationships among nodes, and to distinguish differences in taxa
588 correlations between these two groups of ponies (Table S6). The structural properties of
589 the S network were slightly greater than the R network, indicating more connections and
590 closer relationships of microbial taxa in the S group. Notably, S co-occurrence network
591 displayed higher levels of betweenness centrality, which measures the number of shortest
592 paths going through a given node, and higher degree levels, which describes the number of
593 neighbors relative to R network. Nodes with the highest degree and betweenness centrality
594 values were identified as key genera in the co-occurrence networks. The keystone genera in S
595 were related to the Clostridiales order (*e.g. Clostridium IV, Roseburia, Nakamurella*) or
596 Spirochaetales (*e.g. Treponema*), whereas R network keystone included members of
597 Clostridiales order (*e.g. Clostridium XIV, Roseburia*) and Bacteroidales (*e.g Alloprevotella*).
598
599 To understand the modifications of the gut environment after the natural infection, feces pH
600 measurements and the fungal, protozoan and bacterial loads in feces were investigated
601 between groups of ponies. There were no differences in pH between the groups at any time
602 point, although feces pH significantly decreased after the onset of patent strongyle infection
603 (Figure S8A). Interestingly, anaerobic fungal loads were higher in the S than in the R group (p
604 < 0.05) with more than 0.5 log of difference at day 43 (Figure S8B), while protozoan loads
605 were lower in S group than in the R group at the same time point (Figure S8C). Bacteria loads
606 were constant throughout the experiment (Figure S8D).
607

3.3. Gut microbiota composition and functions shifted immediately after natural
parasite infection
610 Data of both groups were pooled together to assess the influence of natural strongyle infection
611 (from day 43 to day 132) on gut microbiota composition, irrespective of the ponies' predicted
612 susceptibility. Analysis of similarities tests demonstrated that microbiota at day 43 were
613 highly dissimilar and significantly divergent from day 92 and day 132 (R=0.197, $p < 0.001$).
614 Interestingly, species richness increased significantly at day 92 and remained high until the
615 end of the experiment (Figure 5A). Similarly, PCoA, CA and Jaccard network demonstrated a
616 high variability in the distribution of microbiota between day 43 and the other points across
617 the natural parasite infection (Figure 4). Consequently, the most significant alterations at
618 genus level were found at 92 gd relative to 43 gd, which included a decrease ($q < 0.05$; Figure
619 5B) in the relative abundances of members of the order Bacteroidales (*e.g. Alloprevotella,*
620 *Petrimonas, Paludibacter*), Clostridiales (*e.g. Clostridium IV, Oscillibacter, Ethanoligenens*)
621 and Proteobacteria (*e.g. Desulfovibrio*). On the other hand, the relative abundances of
622 dominant genera such as *Clostridium XIVa, Fibrobacter, Ruminococcus, Treponema* and of
623 the members of the as yet unclassified family *Lachnospiraceae* were significantly increased
624 ($q < 0.05$, Figure 6B). The complete list of increased and decreased genera including
625 direction, coefficient and q-values is presented in Supplementary Table S7. These temporal
626 changes on gut microbiota between day 43 and day 132 correlated with an increase in
627 strongyle egg counts and an improvement in pasture quality with less non-digestible
628 carbohydrate components and more N and mineral content (Figure S2A).

13

629
630   These microbiota alterations had an effect on a broad range of biological functions. A total of
631   94 pathways displayed significantly different abundance (50% related to metabolism)
632   between 43 and 92 gd. Interestingly, bacterial invasion of epithelial cells was among the top
633   enriched pathways at day 92 ($q < 0.0003$; Table S8). Conversely, only 34 pathways were
634   found to be different between 92 and 132 gd. Similarly, 50% of the different metabolic
635   potentials were related to metabolism, including amino acid, energy, carbohydrate, lipid and
636   xenobiotic metabolism.
637

638   **4. Discussion**
639   While alternative control strategies are needed for a more sustainable control of horse
640   strongyle infection, the factors contributing to the over-dispersed distribution of these
641   parasites in their hosts remain poorly characterized (Debeffe et al., 2016; Kornaś et al., 2015;
642   Wood et al., 2012). In their preferred niche, strongyles are surrounded by gut microbiota and
643   reciprocal interactions between them are expected. Our study aimed to identify the
644   consequences of parasite infection on the gut microbiota and host physiology under natural
645   conditions and to seek for a metagenomics signature of strongyle infection in resistant and
646   susceptible ponies. Notably, R and S ponies showed contrasted immune responses toward
647   natural strongyle infection, and their gut microbiota displayed variations at the genus level.
648   Additionally, we showed that besides the host susceptibility to strongyle infection, variations
649   in gut microbiota occurred after the onset of strongyle egg excretion during, expanding earlier
650   observations on the association between parasites and gut microbiota composition on other
651   species (Aivelo and Norberg, 2017; Cooper et al., 2013; Ramanan et al, 2016; El-Ashram and
652   Suo, 2017; Fricke et al., 2015; Houlden et al., 2015; Li et al., 2011, 2012; McKenney et al.,
653   2015; Newbold et al., 2017; Osborne et al., 2015; Reynolds et al., 2014b; Su et al., 2017;
654   Walk et al., 2010; Wu et al., 2012; Zaiss et al., 2015; Zaiss and Harris, 2016). Moreover, for
655   the first time we reported the effect of intestinal parasites have on the gut microbiota in
656   horses.
657

658   Under our experimental setting, the combined heat wave and the associated reduced pasture
659   yield and quality induced a mixture of different stresses during the first 43 days of the
660   experiment. Under these challenging climatic and nutritional conditions, R ponies displayed
661   higher levels of eosinophils and monocytes from 24 to 43 gd in comparison to the S ponies.
662   Eosinophilia has been reported in experimentally challenged horses (Murphy and Love,
663   1997). However, no larvae were recovered from pasture samples in our study suggesting mild,
664   if any, contamination, in line with the drought conditions that are detrimental to their survival
665   (Nielsen et al., 2007). In addition, the mild residual egg excretion observed after 24 grazing
666   days occurred in only two susceptible ponies, which cannot explain the increased eosinophils
667   in the R group. Therefore, this differential profile in immune cell populations may result from
668   the stressful environmental conditions as already reported elsewhere (Collier et al., 2008).
669   Remarkably, the contrast between R and S ponies was also found while comparing their
670   respective gut microbiota composition. Although the constituent phyla and genera within the
671   gut microbiota of R and S ponies were congruent with other studies based on horses (Costa et
672   al., 2012, 2015; Mach et al., 2017; Shepherd et al., 2012; Steelman et al., 2012; Venable et al.,
673   2017; Weese et al., 2015), *e.g.* members of Firmicutes, Bacteroidetes, Spirochaetes and
674   Fibrobacteres predominating, R ponies presented an increase of several Clostridiales and
675   Bacteroides species at day 24, whereas only species related to *Blautia* and *Paraprevotella*
676   genera were relatively more abundant in the S. Indisputably, individuals with different
677   susceptibility to parasite infection adapt to environmental stress in different ways. Whether
678   the gut microbiota differences are ascribed to divergence in the immune response or are due to

14

679   impaired nutrient availability remains unclear, but micronutrient deficiencies might dictate
680   microbial-microbial as well as microbial-environmental interactions through the gut (Mach
681   and Clark, 2017).
682
683   The most interesting findings brought forward by this work were obtained during the natural
684   strongyle infection, from day 43 to 132 of the experiment (Figure 6A). Congruent with our
685   initial hypothesis, the observed FEC matched the predicted resistance levels throughout the
686   trial, hence supporting the high reproducibility of FEC (Debeffe et al., 2016; Scheuerle et al.,
687   2016) and the feasibility to select for more resistant individuals (Kornaś et al., 2015).
688   Observed FEC were associated with differing immune responses characterized by higher
689   eosinophil and monocyte counts in R ponies and increased levels of circulating
690   lymphocytes in S ponies during the infection, suggesting a direct functional relationship
691   between parasite infection and immune response (Howitt et al., 2016). The induction of
692   lymphocytes in S animals could have been a way to neutralize invading L3 and facilitate
693   repair and turnover of injury tissue. In R, the eosinophilia, which is a well-recognized
694   immune response to strongyle infection in horses (Reynolds et al., 2012) and plays an
695   important role in destroying parasites by acting as a killer cell against larvae (Herbert et al.,
696   2000), likely played a role in parasitic infection resistance (Lyons et al., 2000). However, the
697   interpretation of the relationship between strongyle infection and immune profile after
698   natural parasite infection in our study required accounting for likely confounding effects of
699   yearly variation in environmental conditions (*e.g.* extreme heat temperatures and reduction
700   of pasture quality).
701
702   Despite the limited infection level monitored throughout the trial, FEC differences between S
703   and R ponies from day 92 to the end of the experiment were also reflected in the composition
704   and function of their gut microbiota. Strongyle natural infection in S ponies coincided with an
705   increase in pathobionts, such as *Pseudomonas, Campylobacter,* and *Bacillus,* anaerobic fungi
706   loads as well as a reduction of commensal genera such as *Clostridium XIVa, Ruminococcus,*
707   and unclassified *Lachnospiraceae* (Figure 6B). Firmicutes belonging to the
708   families *Ruminococcaceae* (also referred as clostridial cluster IV)
709   and *Lachnospiraceae* (also referred as clostridial cluster XIVa) comprise most of the
710   butyrate-producing bacteria in the human gut (Geirnaert et al., 2017). Due to butyrate's
711   anti-inflammatory properties, it might be suggested that the higher helminth infection in
712   susceptible ponies alters the abundance of butyrate-producing bacteria which therefore
713   modulates the gut inflammation (Li et al., 2016). Additionally, the reduced abundance of
714   *Clostridium XIV* in S ponies could have had functional importance for immune gardening
715   against the overgrowth of pathobionts such as *Pseudomonas* and *Campylobacter*. *Clostridium*
716   *XIVa* is one of the main methane-producing bacteria that has been implicated in the
717   maintenance of mucosal homeostasis and protection against intestinal inflammatory diseases
718   through the promotion of T_{reg} cell accumulation (Atarashi et al., 2011). In addition, it was
719   notable that a significant number of microbiota functional pathways in S ponies reflected
720   immunological mechanisms, including pathogen sensing, changes in lipids, and activation of
721   signal transduction pathways inside of the cell that are critical for regulation of immune
722   system and maintaining energy homeostasis (Vassart and Costagliola, 2011).
723
724   Altogether, our data suggest that parasitic infections in S ponies increased the risk of
725   subsequent pathobionts overgrowth in the gut by reducing butyrate producing bacteria that
726   may play an important role in mediating interactions between the host immune system and
727   intestinal parasites (Oliver et al., 2003). Although the mechanisms of the interactions between
728   these specific gut genera and the host require further elucidation, our findings suggest that

15

729   specific modulations of the gut microbiota might be an effective strategy for managing
730   parasite infections in horse.
731
732   The concomitant increase in fungi abundance in S ponies during the natural parasite infection,
733   could have had an important pathophysiological consequence, especially in host fiber
734   metabolism (Dougal et al., 2013) and inflammation (Noverr and Huffnagle, 2004). Fungi have
735   been found to play a significant role in degrading cellulose and other plant fibers making
736   them more accessible to bacteria (Güiris et al., 2010; Leng et al., 2011). This results in a
737   consequent increase in SCFA such as acetate, butyrate and propionate (Ericsson et al., 2016;
738   Nedjadi et al., 2014) which contribute to 60-70% of energy for horses (Al Jassim and
739   Andrews, 2009). Consequently, the fungi-mediated increase in SCFA of microbial origin
740   could have compensated for the decreased abundance of *Ruminococcus* in S ponies. The key
741   contribution of *Treponema*, a non-pathogenic carbohydrate metabolizer (Han et al.,
742   2011), to the co-occurrence network of S ponies at day 92 also suggests that compensatory
743   mechanisms were induced to degrade fiber and supply the host with micro and
744   macronutrients. More detailed nutritional determinations are needed to resolve this issue.
745   Fungi can also secrete inflammatory substances that have been shown to reduce T_{reg} cell
746   responses and may elicit a Th17 innate immune responses and pro-inflammatory cytokines
747   secretion (reviewed by Underhill and Iliev (2014)). In line with the seemingly symbiotic
748   relationship between *H. polygyrus* and bacteria from the family *Lactobacillaceae* in mice
749   (Reynolds et al., 2015), it could be speculated that strongyle and fungi may contribute to each
750   other's success in the ecological niche of the equine intestines.
751
752   Interestingly, R and S ponies exhibited some contrasting phenotypes from the beginning of
753   the experiment under worm-free conditions. Indeed, the predicted R ponies displayed higher
754   levels of circulating monocytes and lower lymphocytes than S ponies at day 0, but they also
755   exhibited higher *Clostridium XIVa, Ruminococcus* and unclassified *Lachnospiracea*
756   abundances and lower abundance of *Acetivibrio*. Because 80% of the ponies from group R
757   presented higher genetic relatedness, we could not exclude the possibility that these specific
758   taxa were influenced by host genetic factors and could sign the intrinsic resistance potential of
759   ponies to strongyle infection. As explained above, *Clostridium XIVa* has been implicated in
760   the maintenance of mucosal homeostasis and the protection against intestinal inflammatory
761   diseases through the promotion of T_{reg} cell accumulation (Atarashi et al., 2011). Therefore, it
762   is tempting to speculate that R and S ponies had an intrinsic different modulation of the
763   mucosal and systemic immunity as well as the gut bacteria composition and function before
764   any infection took place.
765
766   Beyond the effects of susceptibility or resistance to strongyle natural infection on gut
767   microbiota composition, our findings are consistent with other studies showing that helminths
768   have the capacity to induce or maintain higher gut microbiota diversity (Giacomin et al.,
769   2016; Lee et al., 2014; Newbold et al., 2017). In addition, we observed that the patterns of gut
770   microbial alterations during parasite infection were overall highly consistent with other
771   studies (Li et al., 2016; McKenney et al., 2015; Reynolds et al., 2014b; Su et al., 2017; Walk
772   et al., 2010). Specifically, the expansion of Clostridiales has been already reported (Ramanan
773   et al., 2016; McKenney et al., 2015; Walk et al., 2010; Zaiss et al., 2015) and the reduction of
774   *Oscillibacter* have been found in pigs infected by *Trichuris suis* (Li et al., 2012; Wu et al.,
775   2012). Nevertheless, we caution that the late microbiota changes from day 43 to day 92 could
776   also reflect the effects of pasture quality improvements. Therefore, we hypothesize that the
777   increased shifts in gut microbiota composition during parasite infection were partially
778   explained by the nematodes inducing an anti-inflammatory environment and diverting

16

779   immune responses away from themselves (Cattadori et al., 2016; Fricke et al., 2015; Reynolds
780   et al., 2014b, 2015; Zaiss and Harris, 2016). This could also be explained by the changes in
781   the microbial-microbial interactions, the contribution of increased levels of N availability and
782   the non-fibrous carbohydrates in the pasture, as well as changes in the microbial-
783   environmental interactions throughout the gut (D'Elia et al., 2009; Midha et al., 2017). In fact,
784   concomitantly to the parasite infection, pH and fungi loads decreased and protozoa loads
785   increased. As a result, survival and proliferation of certain microbial species become favored
786   or depleted.
787
788   In conclusion, we showed that host parasite susceptibility correlated with parasite burden,
789   with susceptible ponies having higher egg excretions than resistant animals throughout the
790   experiment. However, due to the low level of helminth infections observed under natural
791   conditions, differences in the immune response and gut microbiota composition between
792   susceptible and resistant animals were modest. Eosinophils and monocytes populations were
793   more abundant in resistant ponies while lymphocytes were less abundant in their blood, which
794   may provide a health benefit relative to susceptible animals. Moreover, susceptible ponies
795   presented a reduction of butyrate-producing bacteria such as *Clostridium XIVa,*
796   *Ruminococcus,* and unclassified *Lachnospiraceae*, which may induce a disruption of the
797   maintenance of mucosal homeostasis, intestinal inflammation and dysbiosis. In line with this
798   hypothesis, an increase in pathobionts such as *Pseudomonas, Campylobacter* and fungi loads
799   were observed in susceptible ponies. Our results therefore suggest that susceptibility to
800   strongyle infection occurs in the presence of host genetic and other innate and gut
801   environmental factors that influence immune response and affect individual risk. This
802   investigation should be followed by experimental work in order to establish the causative
803   reasons for variation in the microbiota.
804
805   **Figures**
806   **Figure 1. Experimental design and sampling**
807   A set of twenty female ponies (10 susceptible (S) and 10 resistant (R) to strongylosis) were
808   selected based on their fecal egg counts history during previous pasture seasons and were kept
809   inside during the winter. In the spring, they were treated with moxidectin, to ensure that they
810   were totally free from gastrointestinal nematodes (even from putative encysted larvae) and
811   were kept indoors for three months. Thereafter, once no more effect of moxidectin treatment
812   was detected, the ponies were moved to a 7.44 ha pasture to start the study. At day 30 of the
813   study, a pyrantel treatment was administered to all the animals in order to reset the residual
814   infections that could interfere in the protocol. A longitudinal monitoring of the parasitism
815   level in each animal was performed through five time points from June to October. At each
816   time point, fecal samples were collected from all ponies on 0, 24, 43, 92 and 132 days after
817   the beginning of the grazing season to carry out fecal egg counts, pH measurements, and
818   microbiota profiling. Blood samples were taken at the same time points to analyze
819   biochemical and hematological parameters. This figure was produced using Servier Medical
820   Art, available from www.servier.com/Powerpoint-image-bank
821
822   **Figure 2. Fecal egg counts and hematological parameters between susceptible and**
823   **resistant animals across time**
824   (A) Boxplot of the log parasite fecal egg counts (eggs/g feces) in susceptible (S) and resistant
825   (R) animals. Purple and green stand for S and R ponies respectively. *, q value < 0.05 for
826   comparison between S and R ponies in each time point; (B) Heatmap of individual egg counts
827   (eggs/g feces) in S and R animals (each row corresponding to one individual) across time
828   (column). In the heatmap, egg count values range from 0 (white) and low (blue) to high

829 values (red); (C) Hematocrit (%) between susceptible (S, violet boxes) and resistant (R, green
830 boxes) animals across time. The quantification of different type of leukocytes: eosinophils
831 (D), monocytes (E), and lymphocytes (F) were described between susceptible (S, violet
832 boxes) and resistant (R, green boxes) animals across time. In all cases, boxes show median
833 and interquartile range, and whiskers indicate 5th to 95th percentile. *, p value < 0.05 for
834 comparison between S and R ponies in each time point.
835
836 **Figure 3. Dynamics of microbiota composition between susceptible and resistant animals**
837 **across time**
838 (A) Area plot representation of the phyla detected in feces between susceptible (S) and
839 resistant (R) animals across time; (B) Area plot representation of the most abundant genera in
840 feces between susceptible (S) and resistant (R) animals across time; (C) Boxplot graph
841 representation of genera significantly affected between S and R animals across time. In all
842 cases, susceptible animals are colored in violet and resistant animals in green. Boxes show
843 median and interquartile range, and whiskers indicate 5th to 95th percentile. *, p value < 0.05
844 for comparison between S and R ponies in each time point.
845
846 **Figure 4. Estimation of the α-diversity indexes and β-diversity insusceptible and**
847 **resistant animals during the natural parasite infection (from day 43 to day 132).**
848 (A) Estimation of the α-diversity indexes in susceptible (S) and resistant (R) during the
849 natural parasite infection (from day 43 to 132). The box color indicates the time point
850 analyzed: (pink=43 d, green=92 d, and darkgreen=132 d); (B) α-diversity indexes between S
851 and R animals during the natural parasite infection. Susceptible animals were colored in violet
852 and resistant animals in green; (C) Principal Coordinate analysis of Unifrac distances to
853 compare fecal communities at the level of genera that differ between S and R animals across
854 natural parasite infection. Both PC axes 1 and 2 were plotted. Together they explained 58.6%
855 of whole variation; (D) Correspondence analyses of Unifrac distances to compare fecal
856 communities at the level of genera that differ between S and R animals across natural parasite
857 infection. Both CA axes 1 and 2 were plotted; (E) Genus-level network representation
858 between ponies across natural parasite infection linked within a specified Jaccard distance of
859 0.85. Two samples were considered "connected" if the distance between them was less than
860 0.85. In all cases, the relative position of points was optimized for the visual display of
861 network properties. The point's shape indicates the susceptibility to strongylosis (triangle:
862 susceptible (S); round: resistant (R)), the node color indicates the time point analyzed:
863 (pink=43 d, green=92 d, and darkgreen=132 d).
864
865 **Figure 5. Longitudinal dynamics of microbiota composition upon natural parasite**
866 **infection.**
867 (A) Estimation of the α-diversity indexes across the natural parasite infection: from day 43 to
868 day 132. The box color indicates the time point analyzed: (pink=43 d, green=92 d, and
869 darkgreen=132 d); (B) Boxplot graph representation of genera significantly affected ($q <$
870 0.05) at day 92 relative to day 43. In all cases, the box color indicates the time point analyzed:
871 pink=43 d, green=92 d, and darkgreen=132 d. Boxes show median and interquartile range,
872 and whiskers indicate 5th to 95th percentile. All genera plotted were statistically significant (q
873 < 0.05) between day 92 and day 43.
874
875 **Figure 6. A model for gut microbiota modifications and their effects on host physiology**
876 **after natural strongyle infection**
877 We hypothesize that natural parasite infection in susceptible ponies increases the release of
878 lymphocytes but decreases the monocytes and eosinophils cell counts. Concomitantly,

18

879 parasite infection induced alterations in bacterial-fungal inter-kingdom, increasing the
880 abundance of *Paludibacter*, *Campylobacter, Bacillus, Pseudomonas, Clostridium III,*
881 *Acetivibrio* and the overall loads of fungi and parasite egg counts in the feces.
882 On the other hand, butyrate producing bacteria such as members of *Ruminococcus,*
883 *Clostridium XIVa* and *Lachnospiraceae* family were found to be depleted in susceptible
884 ponies, but enriched in resistant animals, suggesting a possible effect of N-butyrate on the
885 protection of inflammation in resistant animals. Because butyrate is a potent inhibitor of
886 inflammation, it is suggested that susceptible ponies are prone to the gut inflammation
887 because of the altered abundance of butyrate-producing bacteria.
888 The lower N-butyrate bacteria abundance was accompanied by a number of microbiota
889 functional pathways that reflected immunological mechanisms, including pathogen sensing,
890 changes in lipids, and activation of signal transduction pathways inside of the cell. This figure
891 was produced using Servier Medical Art, available from www.servier.com/Powerpoint-
892 image-bank
893
894 **Conflict of Interest Statement**
895 The authors declare that the research was conducted in the absence of any commercial or
896 financial relationships that could be construed as a potential conflict of interest.
897
898 **Authors and Contributors**
899 AB, GS and NM designed the experiment. AC, GS and NM drafted the main manuscript text.
900 NM designed and carried out the bioinformatics and biostatistical analyses, prepared all the
901 figures and provided critical feedback on content. VB performed the RT-qPCR analyses. FR
902 was in charge of pony maintenance and care throughout the experiment and managed
903 sampling. AM analyzed the chemical composition of the diet. JC and CK performed fecal egg
904 counts. MR performed the blood analysis. All authors reviewed the manuscript and approved
905 the final version.
906

920
921 **List of abbreviations**
922 ADF = acid detergent fiber
923 ADL = acid detergent lignin
924 AFNOR = Association Française de Normalisation
925 ANOSIM = analysis of similarities
926 ANOVA= Analysis of the variance
927 CA = correspondence analysis
928 DM=dry matter

929   FEC= fecal egg counts
930   KEGG = Kyoto Encyclopedia of Genes and Genomes
931   NDCS = neutral detergent soluble carbohydrate
932   NDF = neutral detergent fiber
933   NFC = Non-fiber carbohydrate
934   NMDS = non-parametric multidimensional scaling
935   OTU = operational taxonomic units
936   PCoA = principal coordinates analysis
937   PERMANOVA = Permutational Multivariate Analysis of Variance
938   PICRUSt = phylogenetic investigation of communities by reconstruction of unobserved states
939   QIIME = Quantitative Insights Into Microbial Ecology
940   qPCR=real time quantitative PCR
941   RDP = Ribosomal Database Project naïve Bayesian classifier
942   SCFA=short chain fatty acids
943
944   **References**

945   AFNOR (1977a). *Dosage de l'azote en vue du calcul de la teneur en protéines brutes. Norme*
946   *Française NF V18-100*. Afnor, Paris, France.
947   AFNOR (1977b). *Dosage des cendres brutes. Norme Française NF V18-101*. Afnor, Paris,
948   France.
949   AFNOR (1982). *Détermination de la teneur en eau. Norme Française NF V18-109*. Afnor,
950   Paris, France.
951   AFNOR (1993). *Produits agricoles et alimentaires. Détermination de la cellulose brute -*
952   *Méthode générale. . Norme Française NF V03-040.* Afnor, Paris, France.
953   AFNOR (1997). *Détermination séquentielle des constituants pariétaux. Norme Française NF*
954   *V18-122*. Afnor, Paris, France.
955   Aivelo, T., and Norberg, A. (2017). Parasite-microbiota interactions potentially affect
956   intestinal communities in wild mammals. *J. Anim. Ecol.*, 1–10. doi:10.1111/1365-
957   2656.12708.
958   Al Jassim, R. A. M., and Andrews, F. M. (2009). The Bacterial Community of the Horse
959   Gastrointestinal Tract and Its Relation to Fermentative Acidosis, Laminitis, Colic, and
960   Stomach Ulcers. *Vet. Clin. North Am. - Equine Pract.* 25, 199–215.
961   doi:10.1016/j.cveq.2009.04.005.
962   Atarashi K, Tanoue T, Shima T, Imaoka A, Kuwahara T, Momose Y, et al. Induction of
963   colonic regulatory T Cells by indigenous *Clostridium* species. (2011) 331:337-341.
964   doi:10.1126/science.1198469.
965   Boyett, D., and Hsieh, M. H. (2014). Wormholes in Host Defense: How Helminths
966   Manipulate Host Tissues to Survive and Reproduce. *PLoS Pathog.* 10, 2–5.
967   doi:10.1371/journal.ppat.1004014.
968   Bucknell, D., Gasser, R., and Beveridge, I. (1995). The prevalence and epidemiology of
969   gastrointestinal parasites of horses in Victoria, Australia. *Int. J. Parasitol.* 25, 711–724.
970   Caporaso, J. G., Kuczynski, J., Stombaugh, J., Bittinger, K., Bushman, F. D., Costello, E. K.,
971   et al. (2010). QIIME allows analysis of high- throughput community sequencing data
972   Intensity normalization improves color calling in SOLiD sequencing. *Nat. Publ. Gr.* 7,
973   335–336. doi:10.1038/nmeth0510-335.
974   Cattadori, I. M., Sebastian, A., Hao, H., Katani, R., Albert, I., Eilertson, K. E., et al. (2016).
975   Impact of helminth infections and nutritional constraints on the small intestine
976   microbiota. *PLoS One* 11, 1–23. doi:10.1371/journal.pone.0159770.
977   Chao, A. S. J. of S. (1984). Nonparametric estimation of the number of classes in a
978   population. *Scand. J. Stat.* 11, 256–270.

979   Cole, J. R., Wang, Q., Cardenas, E., Fish, J., Chai, B., Farris, R. J., et al. (2009). The
980   Ribosomal Database Project: Improved alignments and new tools for rRNA analysis.
981   *Nucleic Acids Res.* 37, 141–145. doi:10.1093/nar/gkn879.
982   Collier, R. J., Collier, J. L., Rhoads, R. P., and Baumgard, L. H. (2008). Invited Review:
983   Genes Involved in the Bovine Heat Stress Response. *J. Dairy Sci.* 91, 445–454.
984   doi:10.3168/jds.2007-0540.
985   Cooper, P., Walker, A. W., Reyes, J., Chico, M., Salter, S. J., Vaca, M., et al. (2013). Patent
986   Human Infections with the Whipworm, Trichuris trichiura, Are Not Associated with
987   Alterations in the Faecal Microbiota. *PLoS One* 8. doi:10.1371/journal.pone.0076573.
988   Corning, S. (2009). Equine cyathostomins: a review of biology, clinical significance and
989   therapy. *Parasit. Vectors* 2, S1. doi:10.1186/1756-3305-2-S2-S1.
990   Costa, M. C., Arroyo, L. G., Allen-Vercoe, E., Stämpfli, H. R., Kim, P. T., Sturgeon, A., et al.
991   (2012). Comparison of the fecal microbiota of healthy horses and horses with colitis by
992   high throughput sequencing of the V3-V5 region of the 16s rRNA gene. *PLoS One* 7.
993   doi:10.1371/journal.pone.0041484.
994   Costa, M. C., Silva, G., Ramos, R. V., Staempfli, H. R., Arroyo, L. G., Kim, P., et al. (2015).
995   Characterization and comparison of the bacterial microbiota in different gastrointestinal
996   tract compartments in horses. *Vet. J.* 205, 74–80. doi:10.1016/j.tvjl.2015.03.018.
997   D'Elia, R., DeSchoolmeester, M. L., Zeef, L. A. H., Wright, S. H., Pemberton, A. D., and
998   Else, K. J. (2009). Expulsion of *Trichuris muris* is associated with increased expression
999   of angiogenin 4 in the gut and increased acidity of mucins within the goblet cell. *BMC*
1000   *Genomics* 10, 492. doi:10.1186/1471-2164-10-492.
1001   Debeffe, L., McLoughlin, P. D., Medill, S. A., Stewart, K., Andres, D., Shury, T., et al.
1002   (2016). Negative covariance between parasite load and body condition in a population of
1003   feral horses. *Parasitology* 143, 983–997. doi:10.1017/S0031182016000408.
1004   DeSantis, T. Z., Hugenholtz, P., Larsen, N., Rojas, M., Brodie, E. L., Keller, K., et al. (2006).
1005   Greengenes, a chimera-checked 16S rRNA gene database and workbench compatible
1006   with ARB. *Appl. Environ. Microbiol.* 72, 5069–5072. doi:10.1128/AEM.03006-05.
1007   Dixon, P. (2003). VEGAN, a package of R functions for community ecology. *J. Veg. Sci.* 14,
1008   927. doi:10.1658/1100-9233(2003)014[0927:VAPORF]2.0.CO;2.
1009   Dougal, K., de la Fuente, G., Harris, P. A., Girdwood, S. E., Pinloche, E., and Newbold, C. J.
1010   (2013). Identification of a Core Bacterial Community within the Large Intestine of the
1011   Horse. *PLoS One* 8. doi:10.1371/journal.pone.0077660.
1012   Edgar, R. C. (2010). Search and clustering orders of magnitude faster than BLAST.
1013   *Bioinformatics* 26, 2460–2461. doi:10.1093/bioinformatics/btq461.
1014   Edgar, R. C., Haas, B. J., Clemente, J. C., Quince, C., and Knight, R. (2011). UCHIME
1015   improves sensitivity and speed of chimera detection. *Bioinformatics* 27, 2194–2200.
1016   doi:10.1093/bioinformatics/btr381.
1017   El-Ashram, S., and Suo, X. (2017). Exploring the microbial community (microflora)
1018   associated with ovine Haemonchus contortus (macroflora) field strains. *Sci. Rep.* 7, 1–
1019   13. doi:10.1038/s41598-017-00171-2.
1020   Ericsson, A. C., Johnson, P. J., Lopes, M. A., Perry, S. C., and Lanter, H. R. (2016). A
1021   microbiological map of the healthy equine gastrointestinal tract. *PLoS One* 11, 1–17.
1022   doi:10.1371/journal.pone.0166523.
1023   Fricke, W. F., Song, Y., Wang, A.-J., Smith, A., Grinchuk, V., Pei, C., et al. (2015). Type 2
1024   immunity-dependent reduction of segmented filamentous bacteria in mice infected with
1025   the helminthic parasite Nippostrongylus brasiliensis. *Microbiome* 3, 40.
1026   doi:10.1186/s40168-015-0103-8.
1027   Geirnaert, A., Calatayud, M., Grootaert, C., Laukens, D., Devriese, S., Smagghe, G., et al.
1028   (2017). Butyrate-producing bacteria supplemented in vitro to Crohn's disease patient

21

1029   microbiota increased butyrate production and enhanced intestinal epithelial barrier
1030   integrity. *Sci. Rep.* 7, 11450. doi:10.1038/s41598-017-11734-8.
1031 Geurden, T., van Doorn, D., Claerebout, E., Kooyman, F., De Keersmaecker, S., Vercruysse,
1032   J., et al. (2014). Decreased strongyle egg re-appearance period after treatment with
1033   ivermectin and moxidectin in horses in Belgium, Italy and The Netherlands. *Vet.*
1034   *Parasitol.* 204, 291–296. doi:10.1016/j.vetpar.2014.04.013.
1035 Giacomin, P., Agha, Z., and Loukas, A. (2016). Helminths and Intestinal Flora Team Up to
1036   Improve Gut Health. *Trends Parasitol.* 32, 664–666. doi:10.1016/j.pt.2016.05.006.
1037 Giles, C. J., Urquhart, K. A., and Longstaffe, J. A. (1985). Larval cyathostomiasis (immature
1038   trichonema induced enteropathy): A report of 15 clinical cases. *Equine Vet. J.* 17, 196–
1039   201. doi:10.1111/j.2042-3306.1985.tb02469.x.
1040 Goodrich, J. K., Waters, J. L., Poole, A. C., Sutter, J. L., Koren, O., Blekhman, R., et al.
1041   (2014). Human genetics shape the gut microbiome. *Cell* 159, 789–799.
1042   doi:10.1016/j.cell.2014.09.053.
1043 Gruner, L., and Raynaud, J. P. (1980). Technique allégée de prélèvements d'herbe et de
1044   numération, pour juger de l'infestation des pâturages de bovins par les larves de
1045   nématodes parasites. *Med. Vet.* 131, 521–529.
1046 Güiris, A. D. M., Rojas, H. N. M., Berovides, A. V., Sosa, P. J., Pérez, E. M. E., Cruz, A. E.,
1047   et al. (2010). Biodiversity and distribution of helminths and protozoa in naturally
1048   infected horses from the biosphere reserve "La Sierra Madre de Chiapas", Mexico. *Vet.*
1049   *Parasitol.* 170, 268–277. doi:10.1016/j.vetpar.2010.02.016.
1050 Han, C., Gronow, S., Teshima, H., Lapidus, A., Nolan, M., Lucas, S., et al. (2011). Complete
1051   genome sequence of Treponema succinifaciens type strain (6091T). *Stand. Genomic Sci.*
1052   4, 361–370. doi:10.4056/sigs.1984594.
1053 Herbert, D. R., Lee, J. J., Lee, N. a, Nolan, T. J., Schad, G. a, and Abraham, D. (2000). Role
1054   of IL-5 in innate and adaptive immunity to larval Strongyloides stercoralis in mice. *J.*
1055   *Immunol.* 165, 4544–51. doi:10.4049/jimmunol.165.8.4544.
1056 Holm, J. B., Sorobetea, D., Kiilerich, P., Ramayo-Caldas, Y., Estellé, J., Ma, T., et al. (2015).
1057   Chronic Trichuris muris infection decreases diversity of the intestinal microbiota and
1058   concomitantly increases the abundance of lactobacilli. *PLoS One* 10, 1–22.
1059   doi:10.1371/journal.pone.0125495.
1060 Houlden, A., Hayes, K. S., Bancroft, A. J., Worthington, J. J., Wang, P., Grencis, R. K., et al.
1061   (2015). Chronic Trichuris muris infection in C57BL/6 mice causes significant changes in
1062   host microbiota and metabolome: Effects reversed by pathogen clearance. *PLoS One* 10.
1063   doi:10.1371/journal.pone.0125945.
1064 Howitt, M.R., Lavoie, S., Michaud, M., Blum, A.M., Tran, S.V., Weinstock, J.V., Gallini,
1065   C.A., Redding, K., Margolskee, R.F., Osborne, L.C. and Artis, D. (2016). Tuft cells,
1066   taste-chemosensory cells,orchestrate parasite type 2 immunityin the gut. *Science* 351,
1067   1329–1333. doi:10.1126/science.aaf1648.
1068 Kornaś, S., Sallé, G., Skalska, M., David, I., Ricard, A., and Cabaret, J. (2015). Estimation of
1069   genetic parameters for resistance to gastro-intestinal nematodes in pure blood Arabian
1070   horses. *Int. J. Parasitol.* 45, 237–242. doi:10.1016/j.ijpara.2014.11.003.
1071 Kuzmina, T. A., Dzeverin, I., and Kharchenko, V. A. (2016). Strongylids in domestic horses:
1072   Influence of horse age, breed and deworming programs on the strongyle parasite
1073   community. *Vet. Parasitol.* 227, 56–63. doi:10.1016/j.vetpar.2016.07.024.
1074 Langille, M. G. I., Zaneveld, J., Caporaso, J. G., McDonald, D., Knights, D., Reyes, J. A., et
1075   al. (2013). Predictive functional profiling of microbial communities using 16S rRNA
1076   marker gene sequences. *Nat. Biotechnol.* 31, 814–21. doi:10.1038/nbt.2676.
1077 Lee, S. C., Tang, M. S., Lim, Y. A. L., Choy, S. H., Kurtz, Z. D., Cox, L. M., et al. (2014).
1078   Helminth Colonization Is Associated with Increased Diversity of the Gut Microbiota.

22

1079   *PLoS Negl. Trop. Dis.* 8. doi:10.1371/journal.pntd.0002880.

1080   Leng, J., Zhong, X., Zhu, R. J., Yang, S. L., Gou, X., and Mao, H. M. (2011). Assessment of
1081   protozoa in Yunnan Yellow Cattle rumen based on the 18S rRNA sequences. *Mol. Biol.*
1082   *Rep.* 38, 577–585. doi:10.1007/s11033-010-0143-x.

1083   Lester, H. E., Bartley, D. J., Morgan, E. R., Hodgkinson, J. E., Stratford, C. H., and
1084   Matthews, J. B. (2013). A cost comparison of faecal egg count-directed anthelmintic
1085   delivery versus interval programme treatments in horses. *Vet. Rec.* 173, 371.
1086   doi:10.1136/vr.101804.

1087   Lester, H. E., and Matthews, J. B. (2014). Faecal worm egg count analysis for targeting
1088   anthelmintic treatment in horses: Points to consider. *Equine Vet. J.* 46, 139–145.
1089   doi:10.1111/evj.12199.

1090   Li, R. W., Li, W., Sun, J., Yu, P., Baldwin, R. L., and Urban, J. F. (2016). The effect of
1091   helminth infection on the microbial composition and structure of the caprine abomasal
1092   microbiome. *Sci. Rep.* 6, 20606. doi:10.1038/srep20606.

1093   Li, R. W., Wu, S., Li, W., Huang, Y., and Gasbarre, L. C. (2011). Metagenome plasticity of
1094   the bovine abomasal microbiota in immune animals in response to ostertagia ostertagi
1095   infection. *PLoS One* 6. doi:10.1371/journal.pone.0024417.

1096   Li, R., Wu, S., Li, W., Navarro, K., Couch, R., Hill, D., et al. (2012). Alterations in the
1097   Porcine Colon Microbiota Induced by the Gastrointestinal Nematode Trichuris suis.
1098   *Infect. Immun.* 80, 2150–2157. doi:2150–2157.

1099   Lichtenfels, J. R., Kharchenko, V. A., and Dvojnos, G. M. (2008). Illustrated identification
1100   keys to strongylid parasites (strongylidae: Nematoda) of horses, zebras and asses
1101   (Equidae). *Vet. Parasitol.* 156, 4–161. doi:10.1016/j.vetpar.2008.04.026.

1102   Lim, M. Y., You, H. J., Yoon, H. S., Kwon, B., Lee, J. Y., Lee, S., et al. (2017). The effect of
1103   heritability and host genetics on the gut microbiota and metabolic syndrome. *Gut* 66,
1104   1031–1038. doi:10.1136/gutjnl-2015-311326.

1105   Lluch, J., Servant, F., Païssé, S., Valle, C., Valière, S., Kuchly, C., et al. (2015). The
1106   characterization of novel tissue microbiota using an optimized 16S metagenomic
1107   sequencing pipeline. *PLoS One* 10, 1–22. doi:10.1371/journal.pone.0142334.

1108   Love, S., Murphy, D., and Mellor, D. (1999). Pathogenicity of cyathostome infection. *Vet.*
1109   *Parasitol.* 85, 113–121.

1110   Lozupone, C., Stomabaugh, J., Gordon, J., Jansson, J., and Knight, R. (2012). Diversity,
1111   stability and resilience of the human gut microbiota. *Nature* 489, 220–230.
1112   doi:10.1038/nature11550.Diversity.

1113   Lyons, E. T., Drudge, J. H., and Tolliver, S. C. (2000). Larval cyathostomiasis. *Vet. Clin.*
1114   *North Am. Equine Pract.* 16, 501–513. doi:10.1016/S0749-0739(17)30092-5.

1115   Lyons, E. T., Tolliver, S. C., and Drudge, J. H. (1999). Historical perspective of
1116   cyathostomes: Prevalence, treatment and control programs. *Vet. Parasitol.* 85, 97–112.
1117   doi:10.1016/S0304-4017(99)00091-6.

1118   Mach, N., and Clark, A. (2017). Micronutrient Deficiencies and the Human Gut Microbiota.
1119   *Trends Microbiol.* 25, 607-610. doi:10.1016/j.tim.2017.06.004.

1120   Mach, N., Foury, A., Kittelmann, S., Reigner, F., Moroldo, M., Ballester, M., et al. (2017).
1121   The effects of weaning methods on gut microbiota composition and horse physiology.
1122   *Front. Physiol.* 8. doi:10.3389/fphys.2017.00535.

1123   Mackie, R. I., and Wilkins, C. A. (1988). Enumeration of anaerobic bacterial microflora of the
1124   equine gastrointestinal tract. *Appl. Environ. Microbiol.* 54, 2155–2160.

1125   Marley, M. G., Meganathan, R., and Bentley, R. (1986). Menaquinone (vitamin K2)
1126   biosynthesis in Escherichia coli: synthesis of o-succinylbenzoate does not require the
1127   decarboxylase activity of the ketoglutarate dehydrogenase complex. *Biochem.* 25, 1304–
1128   1307.. 1304–1307.

Matthews, J. B. (2014). Anthelmintic resistance in equine nematodes. *Int. J. Parasitol. Drugs Drug Resist.* 4, 310–315. doi:10.1016/j.ijpddr.2014.10.003.

McKenney, E. A., Williamson, L., Yoder, A. D., Rawls, J. F., Bilbo, S. D., and Parker, W. (2015). Alteration of the rat cecal microbiome during colonization with the helminth Hymenolepis diminuta. *Gut Microbes* 6, 182–193. doi:10.1080/19490976.2015.1047128.

Mcmurdie, P. J., and Holmes, S. (2012). Phyloseq: a bioconductor package for handling and analysis of high-throughput phylogeneticsequence data. *Pac. Symp. biocomput.* 235–246.

Midha, A., Schlosser, J., and Hartmann, S. (2017). Reciprocal Interactions between Nematodes and Their Microbial Environments. *Front Cell Infect Microbiol* 7, 144. doi:10.3389/fcimb.2017.00144.

Murphy, D., and Love, S. (1997). The pathogenic effects of experimental cyathostome infections in ponies. *Vet. Parasitol.* 70, 99–110. doi:10.1016/S0304-4017(96)01153-3.

Navas-Molina J, Peralta-Sánchez J, González A, McMurdie PJ, Vázquez-Baeza Y, X Zhenjiang, et al. Advancing our understanding of the human microbiome using QIIME. Methods Enzymol (2013) 74: 371-444. doi:10.1016/B978-0-12-407863-5.00019-8.Advancing

Nedjadi, T., Moran, A. W., Al-Rammahi, M. a, and Shirazi-Beechey, S. P. (2014). Characterization of butyrate transport across the luminal membranes of equine large intestine. *Exp. Physiol.* 99, 1335–1347. doi:10.1113/expphysiol.2014.077982.

Newbold, L. K., Burthe, S. J., Oliver, A. E., Gweon, H. S., Barnes, C. J., Daunt, F., et al. (2017). Helminth burden and ecological factors associated with alterations in wild host gastrointestinal microbiota. *ISME J.* 11, 663–675. doi:10.1038/ismej.2016.153.

Nicholson, J. K., Holmes, E., Kinross, J., Burcelin, R., Gibson, G., Jia, W., et al. (2012). Metabolic Interactions. 108, 1262–1268. doi:10.1126/science.1223813.

Nielsen, M. K., Kaplan, R. M., Thamsborg, S. M., Monrad, J., and Olsen, S. N. (2007). Climatic influences on development and survival of free-living stages of equine strongyles: Implications for worm control strategies and managing anthelmintic resistance. *Vet. J.* 174, 23–32. doi:10.1016/j.tvjl.2006.05.009.

Nielsen, M. K., Vidyashankar, A. N., Olsen, S. N., Monrad, J., and Thamsborg, S. M. (2012). Strongylus vulgaris associated with usage of selective therapy on Danish horse farms-Is it reemerging? *Vet. Parasitol.* 189, 260–266. doi:10.1016/j.vetpar.2012.04.039.

Noverr, M. C., and Huffnagle, G. B. (2004). Does the microbiota regulate immune responses outside the gut? *Trends Microbiol.* 12, 562–568. doi:10.1016/j.tim.2004.10.008.

Ogbourne, C. (1976). The prevalence, relative abundance and site distribution of nematodes of the subfamily Cyathostominae in horses killed in Britain. *J. Helminthol.* 50, 203–214.

Oliver, K. M., Russell, J. A., Moran, N. A., and Hunter, M. S. (2003). Facultative bacterial symbionts in aphids confer resistance to parasitic wasps. *Proc. Natl. Acad. Sci. U. S. A.* 100, 1803–7. doi:10.1073/pnas.0335320100.

Osborne Lisa, Monticelli Laurel, Nice Timothy, Sutherland Tara, S. M., R, H. M., Vesselin, T., Dmytro, K., and Sara, R. (2015). Virus-helminth co-infection reveals a microbiota-independent mechanism of immuno-modulation. *Science* 345, 578–582. doi:10.1126/science.1256942.Virus-helminth.

Peachey, L. E., Jenkins, T. P., and Cantacessi, C. (2017). This Gut Ain't Big Enough for Both of Us. Or Is It? Helminth-Microbiota Interactions in Veterinary Species. *Trends Parasitol.* 33, 619-632. doi:10.1016/j.pt.2017.04.004.

Price, M. N., Dehal, P. S., and Arkin, A. P. (2010). FastTree 2 - Approximately maximum-likelihood trees for large alignments. *PLoS One* 5. doi:10.1371/journal.pone.0009490.

Ramanan, D., Bowcutt, R., Lee, S., Tang, M., Kurtz, Z., Ding, Y., et al. (2016). Helminth Infection Promotes Colonization Resistance via Type 2 Immunity. *Science* 352, 608–

1179   612.
1180 Ramayo-Caldas, Y., Mach, N., Lepage, P., Levenez, F., Denis, C., Lemonnier, G., et al.
1181   (2016). Phylogenetic network analysis applied to pig gut microbiota identifies an
1182   ecosystem structure linked with growth traits. *ISME J.* 10, 2973–2977.
1183   doi:10.1038/ismej.2016.77.
1184 Raynaud, J. P. (1970). Etude de l'efficacité d'une technique de coproscopie quantitative pour
1185   le diagnostic de routine et le con- trole des infestations parasitaires des bovins, ovins,
1186   equines et porcins. *Ann. Parasitol.* 45, 321–342.
1187 Reinemeyer, C. R., Prado, J. C., and Nielsen, M. K. (2015). Comparison of the larvicidal
1188   efficacies of moxidectin or a five-day regimen of fenbendazole in horses harboring
1189   cyathostomin populations resistant to the adulticidal dosage of fenbendazole. *Vet.*
1190   *Parasitol.* 214, 100–107.
1191 Reverter, A., and Chan, E. K. F. (2008). Combining partial correlation and an information
1192   theory approach to the reversed engineering of gene co-expression networks.
1193   *Bioinformatics* 24, 2491–2497. doi:10.1093/bioinformatics/btn482.
1194 Reynolds, L. A., Filbey, K. J., and Maizels, R. M. (2012). Immunity to the model intestinal
1195   helminth parasite Heligmosomoides polygyrus. *Semin. Immunopathol.* 34, 829–846.
1196   doi:10.1007/s00281-012-0347-3.
1197 Reynolds, L. A., Finlay, B. B., and Maizels, R. M. (2015). Cohabitation in the Intestine:
1198   Interactions among Helminth Parasites, Bacterial Microbiota, and Host Immunity. *J.*
1199   *Immunol.* 195, 4059–4066. doi:10.4049/jimmunol.1501432.
1200 Reynolds, L. A., Harcus, Y., Smith, K. A., Webb, L. M., Hewitson, J. P., Ross, E. A., et al.
1201   (2014a). MyD88 signaling inhibits protective immunity to the gastrointestinal helminth
1202   parasite Heligmosomoides polygyrus. *J Immunol* 193, 2984–2993.
1203   doi:10.4049/jimmunol.1401056.
1204 Reynolds, L. A., Smith, K. A., Filbey, K. J., Harcus, Y., Hewitson, J. P., Redpath, S. A., et al.
1205   (2014b). Commensal-pathogen interactions in the intestinal tract lactobacilli promote
1206   infection with, and are promoted by, helminth parasites. *Gut Microbes* 5, 522–532.
1207   doi:10.4161/gmic.32155.
1208 Rideout, J. R., He, Y., Navas-Molina, J. a, Walters, W. a, Ursell, L. K., Gibbons, S. M., et al.
1209   (2014). Subsampled open-reference clustering creates consistent, comprehensive OTU
1210   definitions and scales to billions of sequences. *PeerJ* 2, e545. doi:10.7717/peerj.545.
1211 Sallé, G., Cortet, J., Bois, I., Dubès, C., Larrieu, C., and Landrin, V. (2017). Risk factor
1212   analysis of equine strongyle resistance to anthelmintics. *IJP Drugs Drug Resist.* 7, 407–
1213   415. doi:10.1016/j.ijpddr.2017.10.007.
1214 Sallé, G., Cortet, J., Koch, C., Reigner, F., and Cabaret, J. (2015). Economic assessment of
1215   FEC-based targeted selective drenching in horses. *Vet. Parasitol.* 214, 159–166.
1216   doi:10.1016/j.vetpar.2015.09.006.
1217 Scheuerle, M. C., Stear, M. J., Honeder, A., Becher, A. M., and Pfister, K. (2016).
1218   Repeatability of strongyle egg counts in naturally infected horses. *Vet. Parasitol.* 228,
1219   103–107. doi:10.1016/j.vetpar.2016.08.021.
1220 Scott, I., Bishop, R. M., and Pomroy, W. E. (2015). Anthelmintic resistance in equine
1221   helminth parasites – a growing issue for horse owners and veterinarians in New Zealand?
1222   *N. Z. Vet. J.* 63, 188–198. doi:10.1080/00480169.2014.987840.
1223 Shannon, C. E. (1997). The mathematical theory of communication. *MD Comput* 14, 306–
1224   317.
1225 Shepherd, M. L., Swecker, W. S., Jensen, R. V., and Ponder, M. A. (2012). Characterization
1226   of the fecal bacteria communities of forage-fed horses by pyrosequencing of 16S rRNA
1227   V4 gene amplicons. *FEMS Microbiol. Lett.* 326, 62–68. doi:10.1111/j.1574-
1228   6968.2011.02434.x.

1229 Smith, M. A., Nolan, T. J., Rieger, R., Aceto, H., Levine, D. G., Nolen-Walston, R., et al.
1230   (2015). Efficacy of major anthelmintics for reduction of fecal shedding of strongyle-type
1231   eggs in horses in the Mid-Atlantic region of the United States. *Vet. Parasitol.* 214, 139–
1232   143. doi:10.1016/j.vetpar.2015.09.025.
1233 Steelman, S. M., Chowdhary, B. P., Dowd, S., Suchodolski, J., and Janečka, J. E. (2012).
1234   Pyrosequencing of 16S rRNA genes in fecal samples reveals high diversity of hindgut
1235   microflora in horses and potential links to chronic laminitis. *BMC Vet. Res.* 8, 231.
1236   doi:10.1186/1746-6148-8-231.
1237 Su, C., Su, L., Li, Y., Long, S. R., Chang, J., Zhang, W., et al. (2017). Helminth-induced
1238   alterations of the gut microbiota exacerbate bacterial colitis. *Mucosal Immunol.*, 1–14.
1239   doi:10.1038/mi.2017.20.
1240 Sugahara, H., Odamaki, T., Hasikura, N., ABE, F., and XIAO, J. (2015). Differences in folate
1241   production by bifidobacteria of different origins. *Biosci. Microbiota, Food Heal.* 34, 87–
1242   93. doi:10.12938/bmfh.2015-003.
1243 Taylor, M. A., Coop, R. L., and Wall, R. L. (2007). Veterinary Parasitology. *Blackwell Publ.*
1244   *UK*.
1245 Underhill, D. M., and Iliev, I. D. (2014). The mycobiota: interactions between commensal
1246   fungi and the host immune system. *Nat. Rev. Immunol.* 14, 405–16. doi:10.1038/nri3684.
1247 Van Soest, P. J., Robertson, J. B., and Lewis, B. A. (1991). Methods for Dietary Fiber,
1248   Neutral Detergent Fiber, and Nonstarch Polysaccharides in Relation to Animal Nutrition.
1249   *J. Dairy Sci.* 74, 3583–3597. doi:10.3168/jds.S0022-0302(91)78551-2.
1250 Vassart, G., and Costagliola, S. (2011). G protein-coupled receptors: mutations and endocrine
1251   diseases. *Nat. Rev. Endocrinol.* 7, 362–372. doi:10.1038/nrendo.2011.20.
1252 Venable, E. B., Fenton, K. A., Braner, V. M., Reddington, C. E., Halpin, M. J., Heitz, S. A., et
1253   al. (2017). Effects of Feeding Management on the Equine Cecal Microbiota. *J. Equine*
1254   *Vet. Sci.* 49, 113–121. doi:10.1016/j.jevs.2016.09.010.
1255 Walk, S. T., Blum, A. M., Ewing, S. A. S., Weinstock, J. V., and Young, V. B. (2010).
1256   Alteration of the murine gut microbiota during infection with the parasitic helminth
1257   Heligmosomoides polygyrus. *Inflamm. Bowel Dis.* 16, 1841–1849.
1258   doi:10.1002/ibd.21299.
1259 Weese, J. S., Holcombe, S. J., Embertson, R. M., Kurtz, K. A., Roessner, H. A., Jalali, M., et
1260   al. (2015). Changes in the faecal microbiota of mares precede the development of post
1261   partum colic. *Equine Vet. J.* 47, 641–649. doi:10.1111/evj.12361.
1262 Wood, E. L. D., Matthews, J. B., Stephenson, S., Slote, M., and Nussey, D. H. (2012).
1263   Variation in fecal egg counts in horses managed for conservation purposes: individual
1264   egg shedding consistency, age effects and seasonal variation. *Parasitology*, 1–14.
1265   doi:10.1017/S003118201200128X.
1266 Wu, S., Li, R. W., Li, W., Beshah, E., Dawson, H. D., and Urban, J. F. (2012). Worm Burden-
1267   dependent disruption of the porcine colon microbiota by trichuris suis infection. *PLoS*
1268   *One* 7. doi:10.1371/journal.pone.0035470.
1269 Xiao, L., Herd, R. P., and Majewski, G. A. (1994). Comparative efficacy of moxidectin and
1270   ivermectin against hypobiotic and encysted cyathostomes and other equine parasites. *Vet.*
1271   *Parasitol.* 53, 83–90.
1272 Zaiss, M. M., and Harris, N. L. (2016). Interactions between the intestinal microbiome and
1273   helminth parasites. *Parasite Immunol.* 38, 5–11. doi:10.1111/pim.12274.
1274 Zaiss, M. M., Rapin, A., Lebon, L., Dubey, L. K., Mosconi, I., Sarter, K., et al. (2015). The
1275   Intestinal Microbiota Contributes to the Ability of Helminths to Modulate Allergic
1276   Inflammation. *Immunity* 43, 998–1010. doi:10.1016/j.immuni.2015.09.012.
1277
1278

Supplementary Material

Supporting tables

Table S1. Summary of study samples and fecal bacterial 16S rRNA gene amplicon sequence datasets

Table S2. The OTU taxonomical assignments and OTU counts in each pony across time

Table S3. Chemical composition of pasture across time.

Table S4. Differences in relative abundance of genera between susceptible (S) and resistant (R) animals across time.

Table S5. Differences in KEGG pathway abundance between susceptible (S) and resistant (R) animals across time. Pathways values across time are represented as %, where normalized counts from a particular pathway is divides by the total number of counts in each sample.

Table S6. Topological properties of co-occurring networks obtained from susceptible and resistant animals at day 92 of the experiment.

Table S7. Differences in relative abundance of genera from day 43 to day 132, regardless of susceptibility to strongyles.

Table S8. Differences in KEGG pathway abundance from day 43 to day 132, regardless of susceptibility to strongyles. Pathways values across time are represented as %, where normalized counts from a particular pathway is divides by the total number of counts in each sample.

Supporting figures
Figure S1. Genetic kinship between the 20 Welsh ponies in the experiment
(A) Heatmap of the historical egg counts (eggs/g feces) in susceptible (S) and resistant (R) animals included in the study. The fecal egg counts values of 4 continuous years were included. In the heatmap, rows represent the animals and columns the different time points analyzed. Not all animals have information for each time point. In the heatmap, red = high values, green = low values of egg counts per g of feces; (B) Violin plot of the historical fecal egg counts of the S and R animals included in the study. The median egg counts /g feces were 800 for S (the mean was 897, the first quartile was 350, and the third quartile was 1,375), whereas the median egg counts /g feces were 0 for R (the mean was 246.1864, the first quartile was 0, and the third quartile was 150); (C); Density plot of historical fecal egg counts values in S and R animals; (D) Pedigree plot. A six-generation pedigree plot is illustrated, with different shapes for male (squares) and female (circles). The shapes are black for the 20 ponies in the study; (E) Heatmap of the kinship coefficient matrix, which assess the genetic resemblance between ponies. Each entry in the matrix is the kinship coefficient between two subjects. Animals are arranged in the order of their genetic relatedness; genetically similar animals are near each other. Note that the diagonal elements did not have values above unity, showing no consanguineous mating in the families. The treatment (susceptible (S) or resistant (R) is delineated below to the animal name. In the heatmap, red = high values of genetic relatedness, white = low values of genetic relatedness.

1329
1330 **Figure S2. Overview of the data analysis in the study**
1331 (A) Effect of parasite susceptibility on gut microbiota composition, parasite egg excretion,
1332 gut-related parameters and host parameters across time.
1333 Step 1: Measurement of the gut microbiota composition between susceptible (S) and resistant
1334 (R) ponies across time. This step involved the analysis of the α-diversity and β-diversity
1335 between S and R ponies across time, as well as the analysis to assess gut genera whose
1336 relative abundances changed between groups across time, the determination of the
1337 corresponding KEGG pathways and the inference of the co-occurrence network.
1338 Step 2: Measurement of the gut related parameters between S and R ponies across time. The
1339 gut parameters included the pH, the fungal, bacteria and protozoan loads, as well as the
1340 number of parasite egg in the feces.
1341 Step 3: Measurement of the host parameters between S and R ponies across time. The host
1342 parameters included the body weight, the daily average gain, hematological and biochemical
1343 parameters in blood.
1344
1345 **Figure S3. Whether and pasture quality throughout the experiment**
1346 (A) Daily precipitation and temperatures recorded at a meteorological station located 14 km
1347 from the experimental pasture. Maximum and minimum temperatures are colored in red and
1348 blue, respectively. Dashed line represents precipitation; (B) Chemical composition (crude
1349 protein (CP), neutral and acid detergent fiber (NDF and ADF), crude fiber (CF), crude ash,
1350 and acid detergent lignin (ADL)) of hay at day 0 and pasture at day 24, 43, 92 and 132. From
1351 day 1 to day 43, the lack of rainfall resulted in significant soil moisture deficits and reduced
1352 growth rates of pasture. This period coincided with the late-flowering stage of the pasture,
1353 when stems and leaves are being depleted of nutrients and herbage maturation and
1354 lignification increases. After day 43, the environmental conditions were eminently favorable
1355 to start a second pasture cycle, with a quick herbage growth, high protein content and lower
1356 fiber content. We observed that herbage protein peaked at day 92, after the intense fall rains
1357 and the increased senescence of green material.
1358
1359 **Figure S4. Hemogram data in susceptible and resistant animals across time.**
1360 The evaluation of the hemogram involved the determination of the hematocrit, total white
1361 blood cell counts, total erythrocyte count, erythrocyte indices and platelet counts.
1362 The determination of the hematocrit (A) and the total white blood cells (B) was performed
1363 between susceptible (S, violet boxes) and resistant (R, green boxes) animals across time. The
1364 quantification of different type of leukocytes: eosinophils (C), monocytes (D), lymphocytes
1365 (E), neutrophils (F) and basophils (G) were described between S and R animals across time.
1366 The values corresponding to red blood cell distribution width (H), microcytic (I) and
1367 macrocytic (J) platelets, as well as microcytic red blood cells (K), and macrocytic red blood
1368 cells (L) were plotted. The red blood cell distribution width is plotted in (L). In all cases,
1369 boxes show median and interquartile range, and whiskers indicate 5th to 95th percentile. *, p
1370 value < 0.05 for comparison between S and R ponies in each time point.
1371
1372 **Figure S5. Performance between susceptible and resistant animals across time**
1373 (A) Boxplot and violin plot representation of body weight (kg) between susceptible (S) and
1374 resistant (R) ponies across time; (B) Boxplot and violin plot representation of average daily
1375 gain (kg) between S and R ponies across time. In all cases, susceptible animals were colored
1376 in violet and resistant animals in green.
1377
1378 **Figure S6**. **Biochemical data in susceptible and resistant animals across time.**
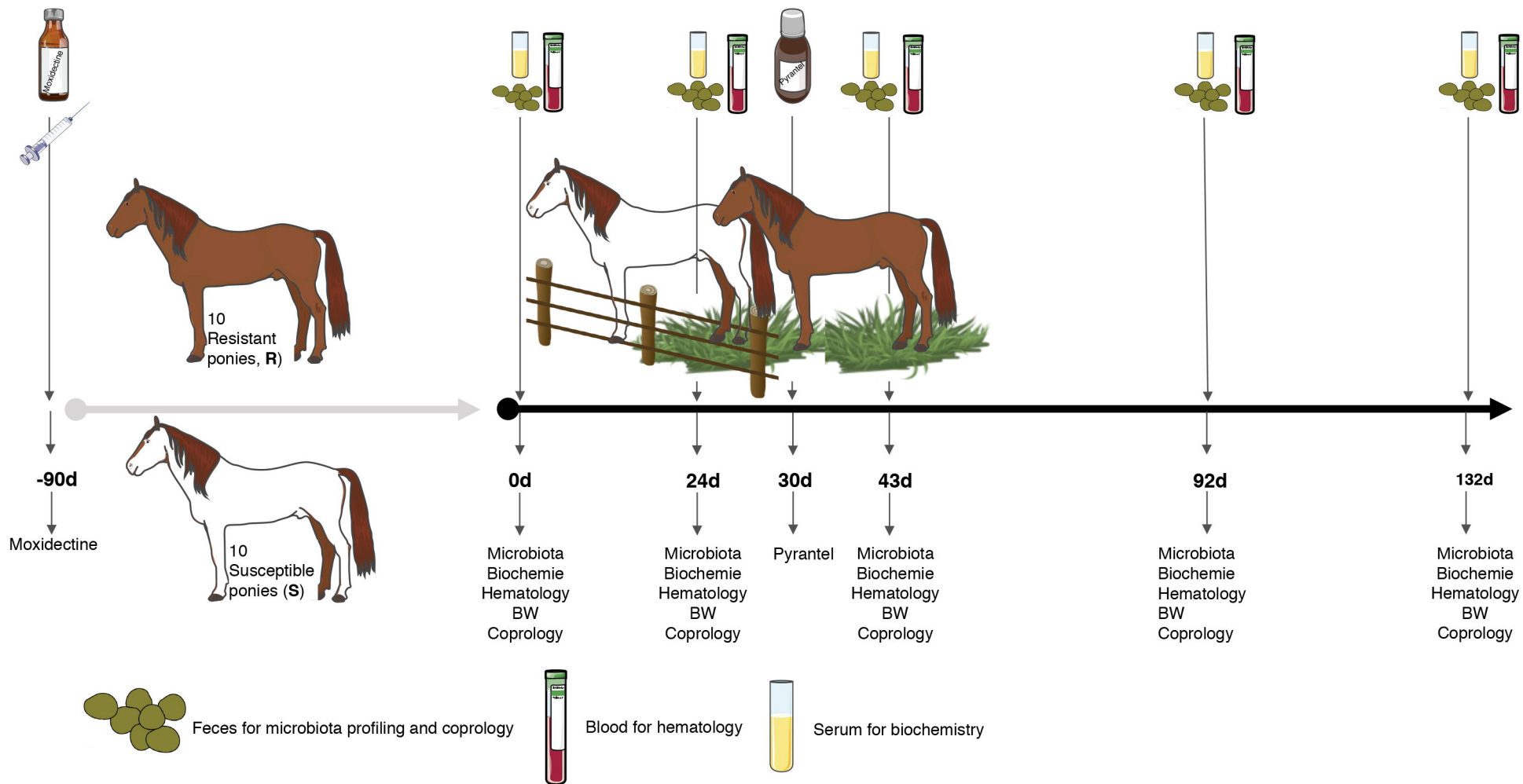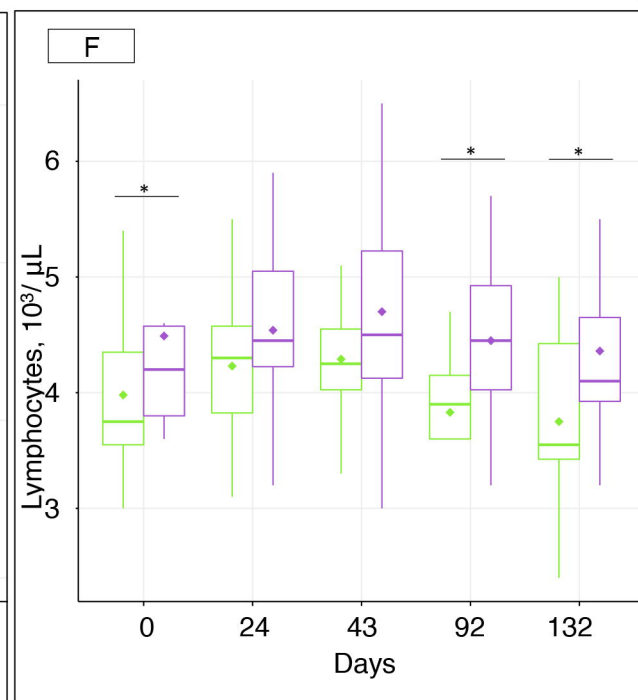
28

1379   Levels of albumin (A), cholesterol (B), globins (C), glucose (D), alkaline phosphatase (E),
1380   ratio albumin/goblins (F), total proteins (G) and urea (H) in susceptible (S, violet boxes) and
1381   resistant animals (R green boxes) were plotted. Boxes show median and interquartile range,
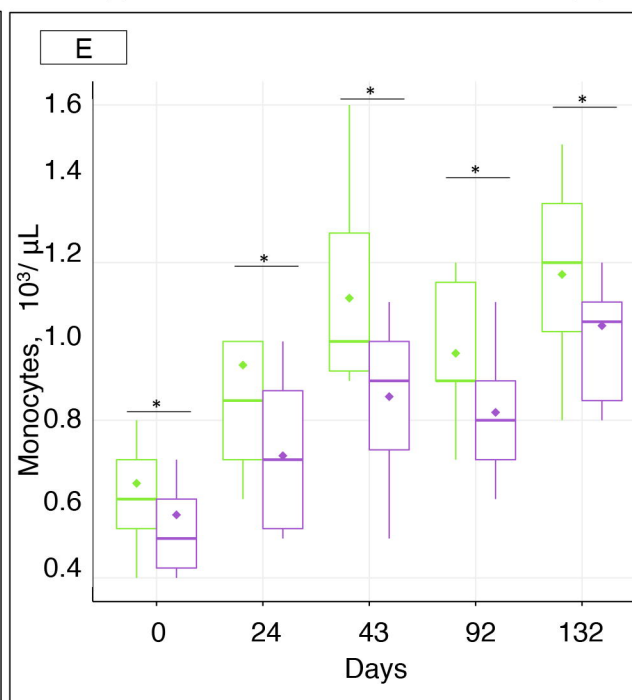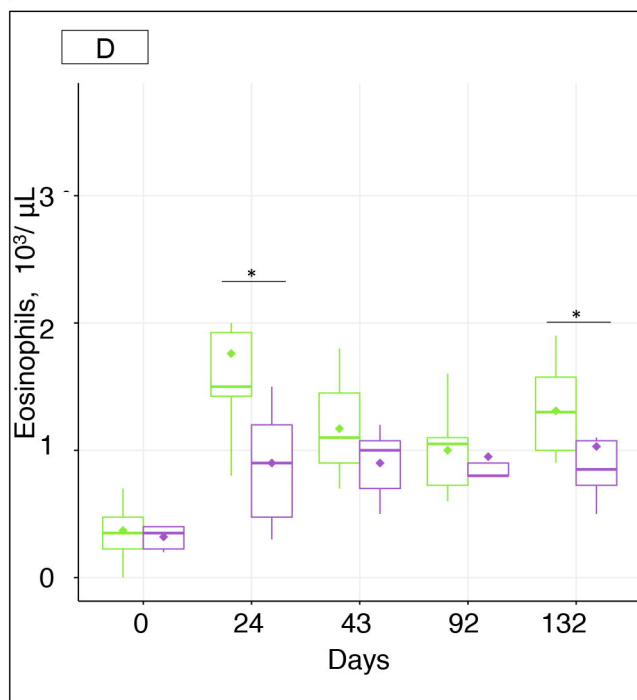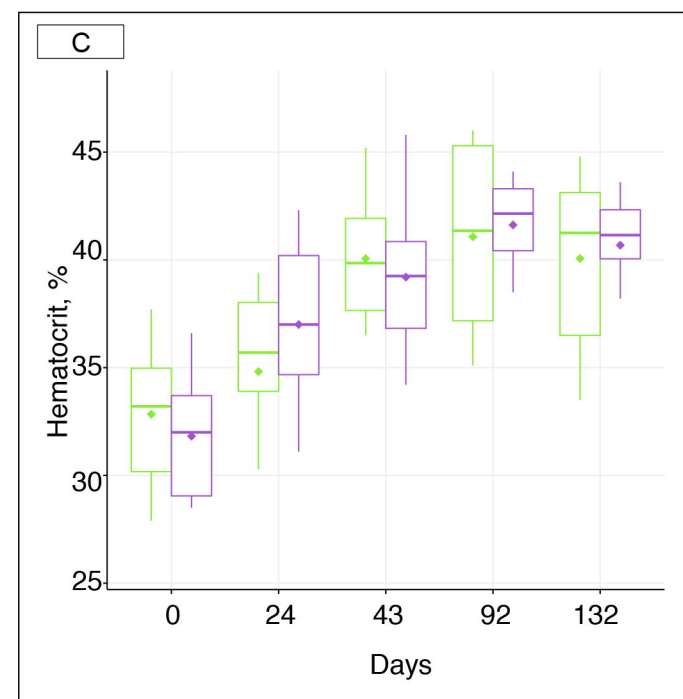1382   and whiskers indicate 5th to 95th percentile. *, p value < 0.05 for comparison between S and
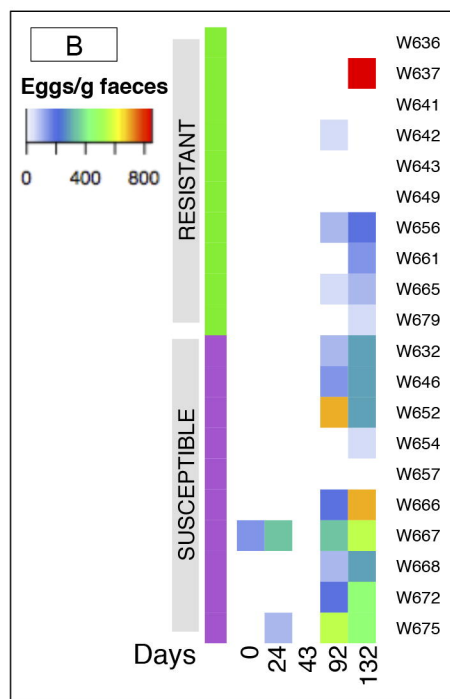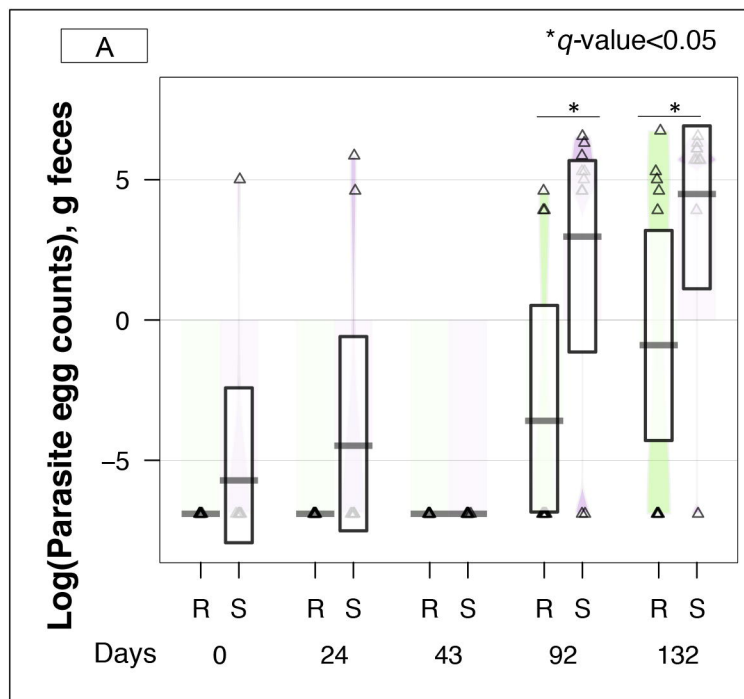1383   R ponies in each time point.
1384
1385   **Figure S7. Co-occurrence network at 92 days after the entry to the pasture for**
1386   **susceptible and resistant ponies**
1387   The correlations among genera were calculated using the PCIT method, which identifies
1388   significant co-occurrence patterns. The size of the node is proportional to genera abundance.
1389   Node fill color corresponds to phylum taxonomic classification. Edges color represent
1390   positive (red) and negative (blue) connections, the edge thickness is equivalent to the
1391   correlation values. Only genera with a relative abundance > 0.10 were included.
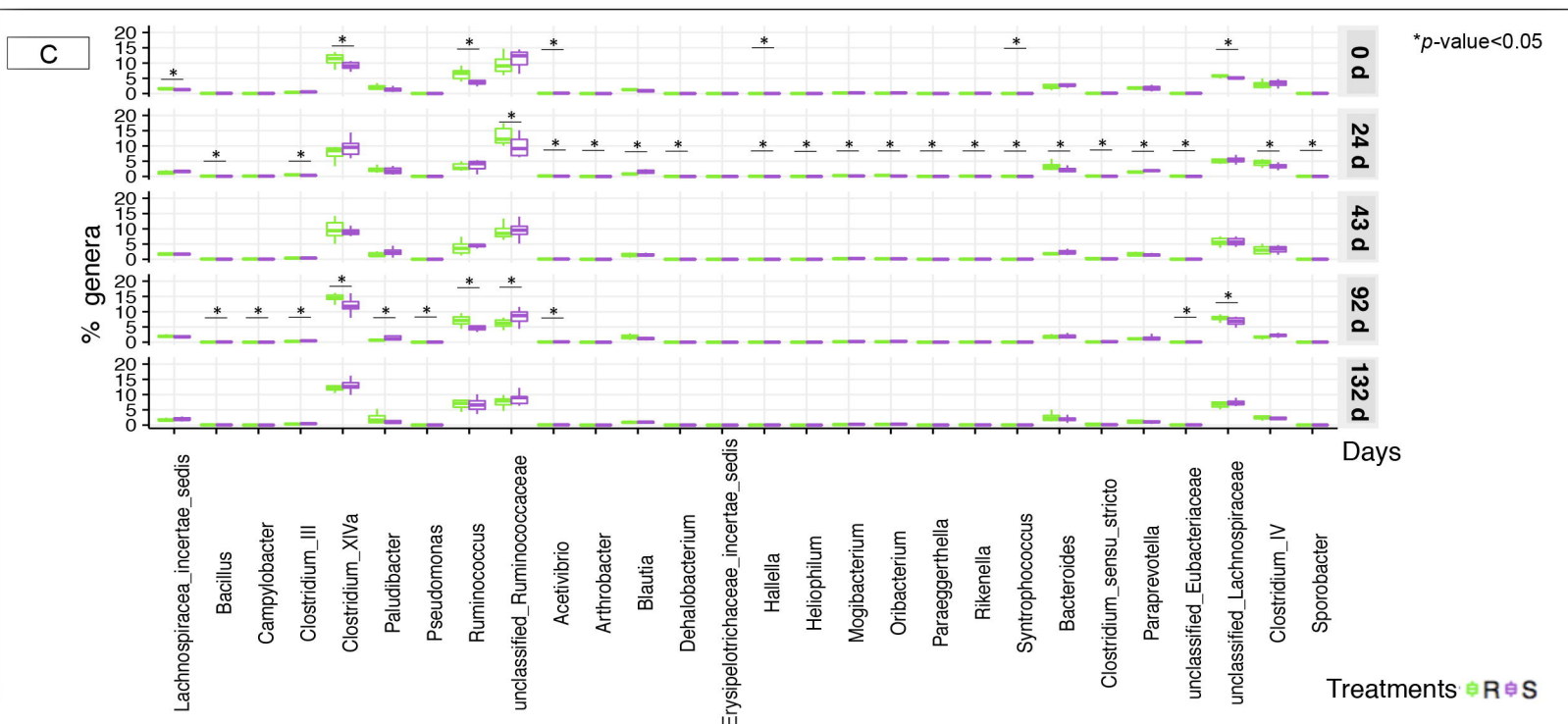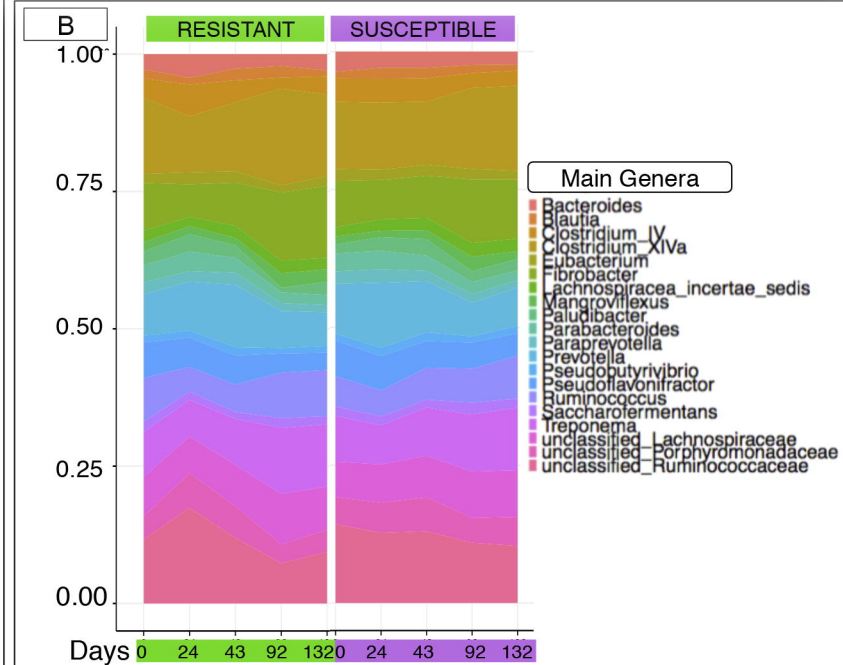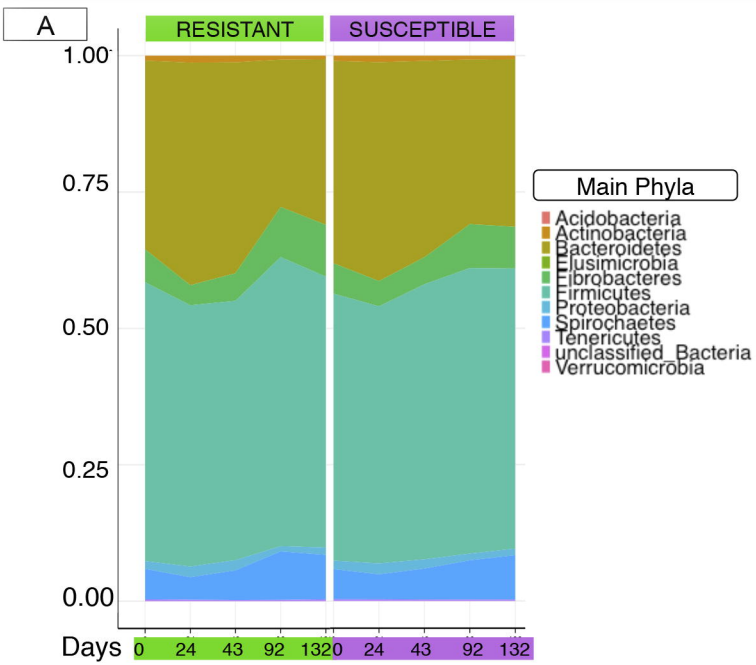1392
1393   **Figure S8. Microbiota functional parameters between susceptible and resistant ponies**
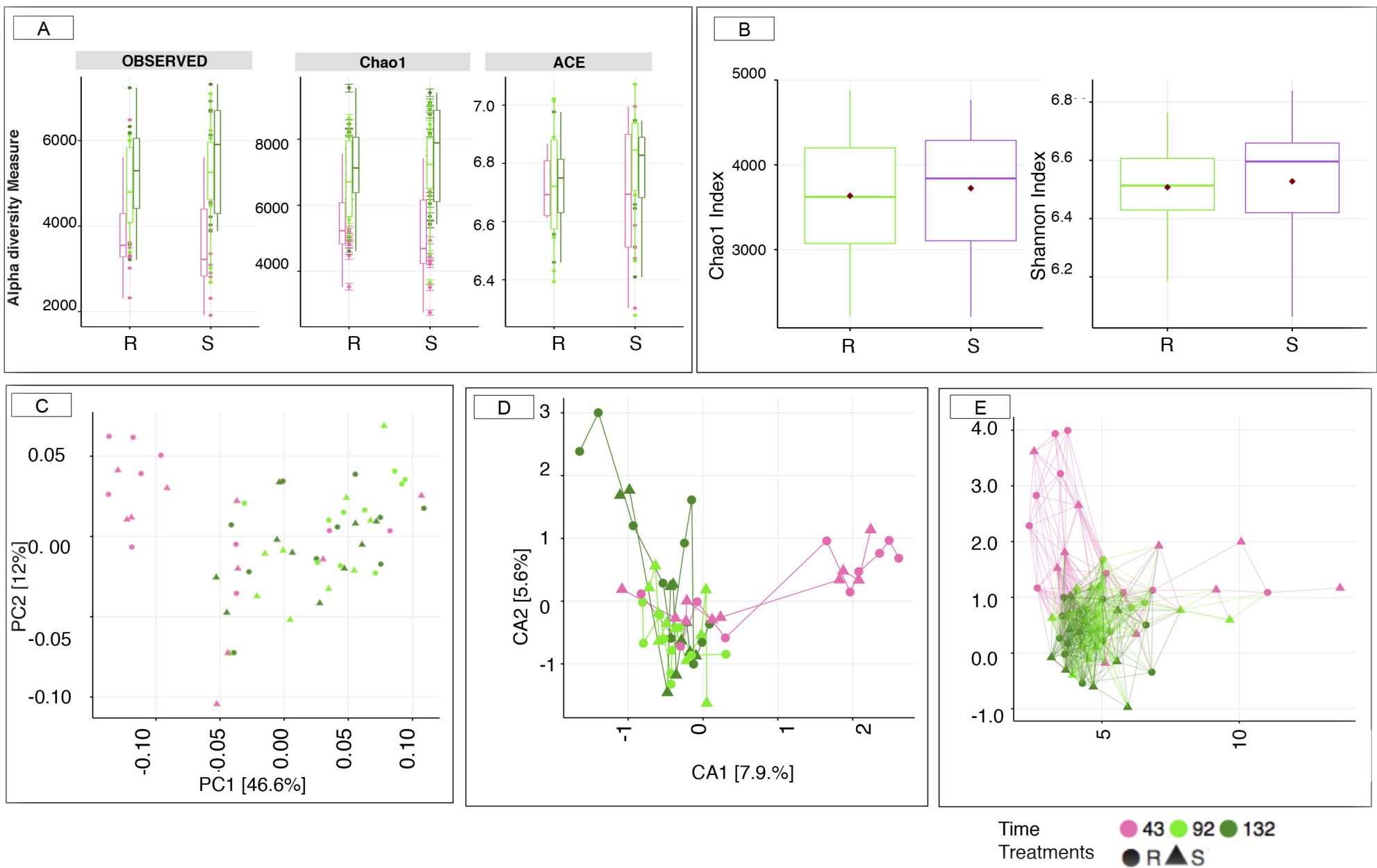1394   **across time.**
1395   (A) Boxplot graph representation of pH in feces between susceptible (S) and resistant (R)
1396   animals at different time points; (B) Boxplot graph representation of loads of anaerobic fungi
1397   in feces between S and R animals at different time points; (C) Boxplot graph representation of
1398   loads of protozoan in feces between S and R animals at different time points; (D) Boxplot
1399   graph representation of loads of bacteria in feces between S and R animals at different time
1400   points. In all cases, susceptible animals are colored in violet and resistant animals in green. *,
1401 p value < 0.05 for comparison between S and R ponies in each time point.

29

-90d

Moxidectine

10 Resistant ponies, **R**)

10 Susceptible ponies (**S**)

0d

Microbiota
Biochemie
Hematology
BW
Coprology

24d

Microbiota
Biochemie
Hematology
BW
Coprology

30d

Pyrantel

43d

Microbiota
Biochemie
Hematology
BW
Coprology

92d

Microbiota
Biochemie
Hematology
BW
Coprology

132d

Microbiota
Biochemie
Hematology
BW
Coprology

Feces for microbiota profiling and coprology

Blood for hematology

Serum for biochemistry

A

OBSERVED | Chao1 | ACE

Alpha diversity Measure

R | S

B

Chao1 Index

R | S

Shannon Index

R | S

C

PC2 [12%]

PC1 [46.6%]

D

CA2 [5.6%]

CA1 [7.9.%]

E

Time: ● 43 ● 92 ● 132
Treatments: ● R ▲ S

A

In the pasture, during summer eggs developed and became infective L3 within 15-30 days. At d43, there is no presence of L3

L5 and mature adults are found in the caecum and colon

Ingested

Eggs passed in feces

Patent period

0d   24d   43d   92d   132d

B

Susceptible	Resistant

circulation   ↑ **Lymphocytes**

Lymphocytes

circulation   ↑ **Monocytes Eosinophils**

Neutorphils   Eosinophils

↑ *Paludibacter*
Campylobacter
Bacillus
Pseudomonas
Clostridium III
Acetivibrio

↑ Fungal loads

↑ Bacterial chemotaxis
Bacterial motility proteins
Bacterial flagellar assembly
Signal transduction
Lipid metabolism
Protein digestion

↑ *Ruminococcus*
Clostridium XIVa
Lachnospiraceae